

PhD Thesis

**IRON OXIDE NANOPARTICLES AND THEIR TOXICOLOGICAL EFFECTS:
IN VIVO AND IN VITRO STUDIES**

Brigitta Szalay

Department of Public Health

Faculty of Medicine

University of Szeged

Szeged

2012

The Applicant's Relevant Publications

- I. Dura Gy, Szalay B. Particle exposure through indoor environment. **Nanotechnology – Toxicological Issues and Environmental Safety**, Springer. 2007. pp 271-276.
- II. Szalay B, Kováčikova Z, Brózik M, Pándics T, Tátrai E. Effects of iron oxide nanoparticles on pulmonary morphology, redox system, production of immunoglobulins and chemokins in rats: In vivo and In vitro studies. **Central European Journal of Occupational and Environmental Medicine** 2008. 14(2): 149-164.
- III. Szalay B, Kováčiková Z, Brózik M, Pándics T, Tátrai E. Vas-oxid nanorészecskék tüdőtoxicitása. **Egészségtudomány** 2009. LIII(1): 103-115.
- IV. Sárközi L, Horváth E, Kónya Z, Kiricsi I, Szalay B, Vezér T, Papp A. Subacute intratracheal exposure of rats to manganese nanoparticles: Behavioral, electrophysiological and general toxicological effects. **Inhalation Toxicology** 2009. 21(S1): 83-91. **IF₂₀₀₉: 3,202**
- V. Szalay B, Tátrai E, Pándics T, Dura Gy. Nikkel-, vas- és cinkoxid nanopartikulumok tüdősejtekre gyakorolt membránkárosító hatása. **Egészségtudomány** 2010. LIV (1): 52-60.
- VI. Szalay B, Vezér T. In vitro mutagenicity evaluation of iron oxide nanoparticles by the bacterial reverse mutation assay. **XVII. International Symposium on Analytical and Environmental Problems**. (Galbács Z., ed.) Szeged, 2011, pp. 275-278.
- VII. Szalay B, Tátrai E, Nyíró G, Vezér T, Dura Gy. Potential toxic effects of iron oxide nanoparticles in in vivo and in vitro experiments. **Journal of Applied Toxicology** 2011. DOI 10.1002/jat.1779. **IF₂₀₁₀: 2,322**

Presentations

- Dura Gy, Szalay B. Particle exposure through indoor environment. Proceedings, pp.3. NATO ARW "Nanotechnology – toxicological issues and environmental security " NATO Advanced Research Workshop Varna, Bulgaria 12 - 17 August 2006.
- Szalay B, Brózik M, Kováčikova Z, Tátrai E. Ferrioxid nanorészecskék tüdőtoxicitása. FHF III. Konferencia, Sopron 2007. május 31 - június 1. (díjazott)
- Tátrai E, Szalay B, Kováčiková Z, Brózik M. How to influence ferric oxide nanoparticles the pulmonary morphology, redox system production of immunoglobulines and chemokines? Toxicological Conference Praga, Czech Republic 11 - 13 June 2007.
- Szalay B, Kováčiková Z, Brózik M, Tátrai E. The effect of ferric oxide nanoparticles on pulmonary morphology, redox system and some immune components. European Respiratory Society Annual Congress Stockholm, Sweden 15 - 19 September 2007.
- Szalay B, Brózik M, Kováčikova Z, Tátrai E. Ferrioxid nanorészecskék tüdőtoxicitása. Magyar Higiénikusok Társasága XXXVII. Vándorgyűlése (FHF III. Konferencián elhangzott, meghívott előadás), Siófok 2007. október 2 - 4.
- Szalay B, Brózik M, Kováčikova Z, Tátrai E. Ferrioxid nanorészecskék hatása a tüdő morfológiájára, immunglobulin termelődésére és kemokin expressziójára. Magyar Toxikológusok Társaságának konferenciája, Eger 2007. október 17 - 19.
- Szalay B, Tátrai E. Nikkel-, vas- és cinkoxid nanopartikulumok hatása tüdősejtekre. FHF IV. Konferencia, Győr 2008. május 29 - 31. (díjazott)
- Sárközi L, Horváth E, Szalay B, Papp A, Vezér T. General and neurotoxicological effects in rats evoked by subacute intratracheal administration of manganese nanoparticles. Magyar Élettani Társaság LXXII. Vándorgyűlése, Debrecen 2008. június 4 - 6.
- Szalay B, Tátrai E. Nikkel-, vas- és cinkoxid nanopartikulumok hatása tüdősejtekre. Magyar Higiénikusok Társaságának XXXVIII. Vándorgyűlése FHF IV. Konferencián elhangzott, meghívott előadás), Balatonvilágos 2008. szeptember 30 - október 2.
- Szalay B, Pándics T. Health effects of iron oxide nanoparticles. DKMT Regional Conference on Environment and Health, Szeged 15 - 16 May 2009.

- Pándics T, Demeter Z, Dura Gy, Szalay B. A nanoanyagok környezetegészségügyi veszélyei és kockázatuk becslésének lehetőségei. Magyar Higiénikusok Társasága XXXIX. Vándorgyűlése, Balatonvilágos 2009. október 6 - 8.
- Szalay B, Oszlanczi G, Nyíró G, Szabó K. Vas(II-III)oxid nanorészecskék toxicitása. FHF VI. Konferencia, Debrecen 2010. május 27 - 29.
- Szalay B, Oszlanczi G, Tátrai E, Szabó Z. Histopathological study of effects of iron oxide nanoparticles in rat. 12th DKMT Regional Conference on Environment and Health, Novi Sad, Serbia 14 - 15 September 2010.
- Szalay B, Tátrai E, Szabó Z. Vas(II-III)oxid nanorészecskék toxikus hatása in vivo és in vitro vizsgálatokban. Magyar Higiénikusok Társasága IX. Nemzeti Kongresszusa, Balatonvilágos 2010. október 5 - 7.
- Oszlanczi G, Hajdú A, Szabó A, Berczi S, Szalay B, Tombácz E. Acute Distribution Of Magnetic Fluids Stabilized By Different Ways Studied In Rats. 11th International Symposium Interdisciplinary Regional Research, Szeged, Hungary 13-15 October 2010.
- Szalay B, Oszlanczi G, Tátrai E, Szabó Z. Vas(II-III)oxid nanorészecskék toxikológiai vizsgálata in vivo és in vitro módszerekkel. Magyar Toxikológusok Társaságának konferenciája, Galyatető 2010. október 13 - 15.
- Dura Gy, Pándics T, Szalay B. Health risk of nanoparticles. From research to regulation. Budapest Millenáris May 2011.
- Szalay B, Szabó Z. Vörösiszap minta vizsgálata in vitro citotoxicitási és Ames tesztben. FHF VII. Konferencia, Esztergom 2011. május 26 - 28. (díjazott)
- Szalay B, Nyíró G, Török G, Szabó Z, Dura Gy. Beszámoló az OKI által szervezett mutagenitási körvizsgálatról. FHF VII. Konferencia, Esztergom 2011. május 26 - 28.
- Szalay B, Nyíró G, Szabó Z. Mutagenic activity of iron oxide nanoparticles in bacterial cells. 13th DKMT Conference on Integrative Medicine, Nutrition and Health. Timisoara, Romania, 08 - 10 September 2011.
- Szalay B, Vezér T. In vitro mutagenicity evaluation of iron oxides nanoparticles by the bacterial reverse mutation assay. XVII. International Symposium on Analytical and Environmental Problems. Szeged, Hungary, 19 September 2011.

Summary

Nanotechnological products called often as a technology of the future used in various fields such as electronics, computer technology, cosmetics industry, in drug delivery or medical diagnostics. These practical applications explain why nanomaterials are arousing great interest in the scientific and economic sphere. At the same time, concerns have arisen in connection with nanomaterials, engineered nanoparticles in particular, having unwanted or unexpected negative impacts on biological systems, resulting in adverse consequences to human and environment. Toxicological examination of nanoparticles (NPs) is essential before we can fully exploit their advantages in practical applications and ensure that potential adverse consequences are minimized.

NPs can enter the human body relatively easily through inhalation, the gastrointestinal tract and the skin. Due to their physicochemical characteristics, they pass the olfactory mucosa, the alveolar and capillary endothelium, or the intestinal endothelium, and reach first the central compartment of the body, and finally the central nervous system after damaging and penetrating the blood brain barrier. The toxicokinetics of NPs has not been elucidated by now, and the most of evidence is based on animal models.

One of the most widely used nanomaterials in biomedical applications (including magnetic drug targeting, hyperthermia and magnetic resonance imaging) are iron oxide NPs. Iron oxide NPs are found naturally in the environment as particulate matter in air pollution and in volcanic eruptions. Either magnetite or maghemite – the two most commonly studied iron oxides – particles can be generated as emissions from traffic, industry and power stations but can also be specifically synthesised chemically for a wide variety of applications (so-called engineered nanoparticles).

The aim of this study was determination the potential, and up to now not completely examined, adverse effects associated with iron oxide NPs following airways exposure, including general and specific toxicological actions (on the respiratory system, immune system and on certain macromolecules). Both *in vivo* animal tests and *in vitro* examinations have notable advantages and disadvantages; but by combining these in a complex experimental model, early detection of possible toxicological effects can be achieved, and new relationships between the primary outcomes can be revealed. This thesis comprises both

in vivo and *in vitro* tests for toxicological examination of iron oxide NPs. We looked for answers to the following questions: 1) Does intratracheal application of iron oxide nanoparticles cause any general toxic effect and histopathological changes in rat organs? 2) Does it cause any toxic effect on rat respiratory system? 3) Does it cause any harmful effect in *in vitro* cell lines? 4) Can mutagenic activity be detected in bacterial cells exposed to iron oxide nanoparticles?

In *in vivo* experiments male rats were treated once intratracheally with 1 and/or 5 mg/ml iron oxide NPs. In Experiment I each group contained 30 animals at start and 6 of the 30 rats per group were sacrificed after 1, 3, 7, 14 and 30 days, respectively. In Experiment II each group contained 24 animals at start and 6 of the 24 rats per group were sacrificed after 1, 3, 7 and 14 days. In Experiment III each group contained 12 animals at start and 6 of the 12 rats per group were sacrificed after 7 and 30 days, respectively.

In Experiment I, body and organ weights were monitored and histopathological analysis was undertaken. Intratracheal instillation of iron oxide NPs caused a significantly slowed body weight gain compared to the control groups. Among the relative organ weights, weight of the lungs decreased significantly with increasing dose and time. Histopathological examination revealed no abnormalities in the exposed rats' organs (lungs, liver, kidneys and spleen) except in the lungs, where the interstitium was widened and a weak pulmonary fibrosis developed by the end of examination period.

In Experiment II, immunological studies were performed. Blood samples were taken from the abdominal aorta and bronchoalveolar lavage (BAL) was carried out with physiological saline. IgA, IgG, and IgM concentrations were determined by the sandwich ELISA (enzyme-linked immunosorbent) assay. 1 mg/ml iron oxide NPs decreased the IgA level in the blood but not in BAL. IgG and IgM (immunoglobulins of peripheral airways) showed significant decrease in BAL whereas they did not alter in the blood.

In Experiment III, effect of iron oxide NPs on pulmonary redox system were examined. The treated animals' lungs were frozen in liquid nitrogen and placed in a freezer. On the day of examination, after homogenisation of the lungs, samples were centrifuged. Total glutathione (GSH) estimation was determined using the GSH reductase method. Extracellular Cu,Zn/superoxide dismutase (EC-SOD) was estimated with the use of a Randox kit. At 7 and 30 days after the iron oxide NPs exposure neither GSH content nor EC-SOD activity could be measured.

In *in vitro* studies effect of iron oxide NPs on primary culture of rat lung cells (alveolar macrophages and type II pneumocytes isolated from male rats) and human A549 cell line, and potential relationship between cell damage and proinflammatory proteins was assessed. Finally, cytotoxic and genotoxic effects of these nanoparticles were studied on Mammalian Vero cell line and bacterial strains, respectively.

In Experiment IV, animal alveolar macrophages, type II pneumocytes and human A549 lung cells were examined by lectin histochemistry assay (for detection of oligosaccharide molecules bound to protein molecules in the cell membranes) and chemokines levels were measured. Lung cells were exposed to iron oxide NPs at doses 1, 5, and 10 µg/ml. At smaller concentrations, the membranes of alveolar macrophages and type II pneumocytes proved to be intact similarly to control, while A549 cells showed incomplete membranes already at 1 µg/ml concentration. At 10 µg/ml concentration the membranes of both animal and human lung cells became irregular and lost continuity, finally the cells were fragmented.

In Experiment V, potential relationship between cell damage and production of chemokines were examined. The primary culture of rat lung cells were exposed to iron oxide NPs at doses 1, 5, and 10 µg/ml. After 24h incubation the supernatants of the cells were collected and sandwich ELISA was used to measure chemokines (MCP-1 and MIP-1α) levels. Iron oxide nanoparticles significantly increased the expression of MCP-1 and MIP-1α in AM. In PII cells, production of MCP-1 significantly increased while MIP-1α significantly decreased.

In Experiment VI, the possible cytotoxic effect of iron oxide NPs were analysed. The NPs were added to the Vero cells at 78, 156, 313, 625, 1250, 2500, 5000 and 10000 µg/ml concentration, and incubated for 4 and 24 hours. Cell viability changed from ca. 100% to approximately 13% with increasing iron oxide NP concentrations.

In Experiment VII, the potential mutagenic effect of iron oxide NPs were tested employing *Salmonella typhimurium* and *Escherichia coli* strains (Ames test). Seven doses of iron oxide NPs (6.9-5000 µg/plate) were tested. The average number of revertant colonies and change in the background growth were similar in the nanoparticle-treated groups and the negative control. None of the revertant rates was greater than or equal to the twofold of the negative controls, and no concentration-dependent increase was observed.

In conclusion, the results of this study and the answers to the questions pointed out as aims of the work can be summarized as follows:

- 1) Acute intratracheal application of iron oxide nanoparticles had evident general toxic effect (altered body and lung weights) and caused specific pathomorphological damage in the treated rats' lungs.
- 2) NPs which reached the lower airways proved to be immunosuppressive: there was decreased immunoglobulin level (IgM and IgG) in the peripheral bronchioles. However, two components of pulmonary redox system (GSH and EC-SOD) did not change, therefore further examination is required.
- 3) The NPs caused irreversible injury to the membranes of alveolar cells. Human A549 cells were more sensitive than animal cells. Our results showed connection between damage of lung cells and production of chemokines. The alveolar epithelial cells could produce chemokines which may regulate inflammatory and immune responses in the alveolar microenvironment. The iron oxide NPs had moderate cytotoxic effect on Vero cell line.
- 4) No mutagenic activity could be observed in the bacterial reverse mutation (Ames) test.
- 5) The new, complex experimental model, comprising both *in vivo* and *in vitro* investigations, proved to be suitable for early detection of (previously unknown or partially documented) toxic effects of iron oxide NPs, and for revealing certain connections between the individual toxic effects.

Our results underline the importance and necessity of further long term toxicological experiments. More attention should be paid on the toxic effects induced by nanoparticles in human beings.

Table of Contents

1	INTRODUCTION.....	1
1.1	Toxicology and nanomaterials.....	1
1.2	Metal oxide nanoparticles.....	5
1.3	Aims of the study.....	10
2	MATERIALS AND METHODS	12
2.1	Iron oxide nanoparticles	12
2.2	<i>In vivo</i> experiments.....	12
2.3	<i>In vitro</i> experiments.....	16
2.4	Statistical analysis.....	20
3	RESULTS.....	21
3.1	<i>In vivo</i> experiments.....	21
3.2	<i>In vitro</i> experiments.....	25
4	DISCUSSION AND CONCLUSION	31
5	REFERENCES.....	35
6	ACKNOWLEDGEMENT	43
7	APPENDIX	44

Abbreviations

2AA	2-aminoanthracene
9AAC	9-aminoacridine
A549	human lung adenocarcinoma cell line
AM	alveolar macrophages
BAL	bronchoalveolar lavage
BET	Brunauer-Emmett-Teller (Brunauer et al, 1938)
DAB	3,3'-diaminobenzidine-4HCl
DMEM	Dulbecco's modified eagle's medium
DMSO	dimethylsulphoxide
FDA	Food and Drug Administration
IONP	iron(II,III)oxide and/or iron(III)oxide nanoparticle
MCP-1	macrophage chemoattractant protein -1
MIP-1 α	macrophage inhibitory protein -1 α
MMS	methymethane sulfonate
MNP	magnetic nanoparticle
MRI	magnetic resonance imaging
NGF	nerve growth factor
NPDA	4-nitro-1,2-phenylenediamine
NP	nanoparticle
OD	optical densities
PII	type II pneumocytes
RES	reticuloendothelial system
RT	room temperature
SAZ	sodium azide
SPION	superparamagnetic iron oxide nanoparticles
TEM	transmission electron microscope

1 INTRODUCTION

1.1 Toxicology and nanomaterials

1.1.1 Toxicology and nanotoxicology

Toxicology is the study of potentially harmful effects of substances on living organisms, and nanotoxicology refers to the study of the potentially harmful effects of nanomaterials, in particular nanoparticles (NPs) (Donaldson et al, 2004). Nanotoxicology focuses upon gaining a thorough understanding of the relationship between the toxicity of NPs depending on their dose levels and physicochemical properties such as size, shape, reactivity and material composition (Paur et al, 2011). Nanomaterials possess structures with dimensions at the nanoscale, while NPs are defined as particles with at least one dimension less than 100 nm. NPs and nanomaterials have been designed and made as part of the recent advances in nanotechnology.

There are hundreds of commercially available products using nanotechnology currently on the market including cosmetics, sunscreens, textiles and sport items, veterinary medicines and so on (PEN, 2005). Roco (2005) predicted four overlapping generations of nanotechnology products from 2000 to 2020. The first generation involved the simple components of NPs, nanotubes, nanolayers and nanocoatings. The second generation (after 2005) involves active nanostructures that change their properties (morphology, shape, magnetic, biological, etc.) during operation. Examples are targeted drugs and chemicals, energy storage devices, transistors and so on. In the third generation (after 2010) includes nanosystems that might self-assemble or self-organise. Examples are artificial organs and electronic devices. The fourth generation (after 2015-2020) includes molecular nanosystems, where each molecule in the nanosystem has a specific structure and plays a different role (Roco, 2005).

1.1.2 Possible benefits and dangers of nanotechnology

Nanotechnology has large potential benefits to a range of areas. Nanomaterials have the potential to improve the environment through the development of new solutions to environmental problems. For example applications of nanomaterials to detect, prevent and remove pollutants (Lee et al, 2005, Kamat and Meisel, 2003) or using nanotechnology to design cleaner industrial process and create environmentally friendly products (Kamat et al, 2002).

Nanotechnology has the potential to improve the life of people in general and especially of those with severe health problems. Such persons can benefit from early diagnoses, treatment and prevention of cancer and other diseases (Cuenca et al, 2006) or continuous health monitoring and semi-automated treatment using small and cheap sensors and other implantable devices (Roco and Bainbridge, 2003).

The rapid growth of nanotechnology industry and its ever increasing applications will inevitably increase the concentration of nanomaterials in the environment, with potential human and environmental exposure as a consequence (EC COM (338), 2004, RSRAE, 2004). The human body is exposed to NPs through four possible routes: inhalation of airborne NPs, ingestion of drinking water or food additives, dermal penetration by skin contact, and injection of engineered nanomaterials (Oberdörster et al, 2005). Regarding the environment, nanomaterials may potentially effect it in three possible ways: (i) direct effect on micro-organisms, invertebrates, fish and other organisms; (ii) interaction with contaminants that may change the bioavailability of toxic compounds and/or nutrients; and (iii) changes to non-living environmental structures (Lead and Smith, 2009).

1.1.3 Exposure, cellular uptake and responses

Nanoparticles are emitted into the environment by primary sources such as natural phenomena, combustion processes or industrial activities (e.g. welding) or are released during generation and handling of engineered NPs. As NPs are transported through the environment, they can be physically (size and shape) and chemically modified due to interactions with sunlight, water and other environmental substances.

Because the lung is considered by far the most important portal of entry for NPs into the human body this overview will mainly focus on the lung as a potential barrier for inhaled NPs. It should however be noted that evidence has been published that nanoparticles can also deposit on the olfactory epithelium and directly be translocated to the brain (Oberdörster et al, 2009).

The amount of NPs contained in the inhaled air is typically referred to as the exposure level. However, the biologically more relevant measure is the (biological) dose, i.e. the amount of particles seen by the biological response (effect) system. For inhalation exposures as considered here the dose refers to the amount of particles reaching the lung epithelium. Once the dose is known one can infer the biological effect from toxicological dose-response measurements using either *in vivo* (animal) or *in vitro* (cell) models (Paur et al, 2011).

The deposition of particles in the lung is size dependent. 90% of inhaled 1 nm particles are deposited in the nasopharyngeal region, only 10% in the tracheobronchial region, and essentially none in the alveolar region. 5 nm particles show about equal deposition of approximately 30% of the inhaled particles in all three regions. 20 nm particles have the highest deposition efficiency in the alveolar region (~ 50%), whereas in tracheobronchial and nasopharyngeal regions this particle size deposits with approximately 15% efficiency. Deposited NPs overcome the tissue barrier as well as the cellular membranes and translocate to extrapulmonary sites and reach other target organs by transcytosis across epithelia of the respiratory tract into the interstitium and access to the blood circulation directly or via lymphatics, resulting in distribution throughout the body (Oberdörster et al, 2005).

Different mechanisms of cellular uptake and intracellular trafficking have been described for NPs: (A) Phagocytosis, an actin-based mechanism occurring primarily in professional phagocytes, leading to phagosomes and phago-lysosomes. (B) Macropinocytosis, also an actin-based pathway, leading to macropinosomes which might be exocytosed or fuse with lysosomes. (C) Clathrin-mediated endocytosis, associated with the formation of a clathrin lattice and depending on the GTPase dynamin, forming primary endosomes and late endosomes including multivesicular bodies. (D) Caveolae-mediated endocytosis, with typical flask-shaped invaginations made of caveolin dimers, also dynamin-dependent and forming caveosomes, which fuse with the endoplasmic reticulum or translocate through the cell. (E) Particle diffusion through the apical membrane, resulting in particles located freely in the cytosol (Paur et al, 2011, Brandenberger et al, 2010). And located inside the cell, certain NPs have been shown to be cytotoxic (Oberdörster et al, 2005). In addition, NPs are also known to cause several biological responses including the generation of reactive oxygen species (Gonzalez-Flecha, 2004), alter cell signaling (Clift et al, 2010), as well as cause an enhanced expression of pro-inflammatory cytokines (Muller et al, 2005) without causing cytotoxicity.

1.1.4 Methods for assessing toxicity of nanomaterials

Toxicity is usually determined by animal experiments according to the guidelines of the OECD (Organization for Economic Cooperation and Development). Various OECD guidelines for testing acute and chronic toxicity are available, depending on the required information. The determination of repeated dose inhalation toxicity requires long term studies ranging from several days up to two years employing large numbers of test animals, followed by extensive examination of tissue samples.

In the year 2005 10 billion euro were spent on animal experiments worldwide and more than 100 million animals were used (Taylor et al, 2008), about 20% of these for toxicological testing. In the interest of limiting the animal experiments to a minimum, widespread toxicity screening should be performed with *in vitro* test methods. Especially the use of cell cultures and organ tissue for *in vitro* studies in modern exposure systems open new avenues for reliable toxicological studies without animals. This screening should be optimized to identify NPs of relative high toxicity. Only those ‘high-hazard’ NPs should then be assessed by animal testing. Dedicated strategies have been developed to reduce the number of animal experiments for the implementation of the European Guideline REACH (Registration, Evaluation and Authorization of Chemicals) (REACH, 2006), which regulates the toxicity testing required for all chemicals used in the European Community. However, it has to be acknowledged that cell and tissue cultures will not be able to replace *in vivo* tests completely, since the complex mammalian organism cannot be represented by cell cultures and since the lifetime of cell cultures is too short to allow for the assessment of chronic toxicity (Paur et al, 2011).

As with any other man-made materials, both *in vivo* and *in vitro* studies on biological effects of NPs need to be performed.

In vitro model systems provide a rapid and effective means to assess NPs for a number of toxicological endpoints. Such studies can be used to establish concentration-effect relationships and the effect-specific thresholds in cells. They also serve as well defined systems for studying the structure-activity relationships involving nanomaterials (Arora et al, 2012). Advantages of *in vitro* methods using various cell lines include: 1) efficiency, rapidity and cost-effectiveness; 2) identification of primary mechanisms of toxicity in the absence of the physiological and compensatory factors that confound the interpretation of whole animal studies; 3) revelation of primary effects of target cells in the absence of secondary effects caused by inflammation; and 4) scope for improvements in design of subsequent expensive whole animal studies (Huang et al, 2010).

Donaldson et al (2009) reported the potential dangers of exclusive use of *in vitro* testing. The authors stated that cells in culture did not experience the range of pathogenic effects that were likely to be observed *in vivo*; which were partly related to issues of translocation, toxicokinetics and coordinated tissue responses. In an article by Dhawan and Sharma (2010) both *in vitro* and *in vivo* toxicity of nanomaterials have been reviewed. The authors discussed interferences in *in vitro* assays (due to the unique physico-chemical properties of NPs), as well as major challenges for *in vivo* assays such as dosimetry, optimization of dispersion,

evaluation of interactions and biodistribution etc. Hence it is essential that multiple assays be employed depending on the type of nanomaterial.

1.2 Metal oxide nanoparticles

Presently, the group of the most important nanomaterials includes simple metal oxides such as titanium oxide (TiO_2), zinc oxide (ZnO), magnesium oxide (MgO), copper oxide (CuO), aluminium oxide (Al_2O_3), manganese oxide (MnO_2) and iron oxide (Fe_3O_4 , Fe_2O_3) (Pan et al, 2010, Fahmy and Cormier, 2009, Balasubramanyam et al, 2010, Sárközi et al, 2009, Oszlánzi et al, 2010, Singh et al, 2010). Metal oxides NPs are finding increasing application in a wide range of fields and represent about one-third of the consumer products nanotechnology market (Maynard, 2006). These materials are used as pigments in paints (TiO_2), as sunscreens and cosmetics (TiO_2 , ZnO), as antimicrobial agents (MgO , CuO), in industrial operations (Al_2O_3 , MnO_2) and for medical purposes (Al_2O_3 , Fe_3O_4 , Fe_2O_3) (Pan et al, 2010, Fahmy and Cormier, 2009, Balasubramanyam et al, 2010, Sárközi et al, 2009, Oszlánzi et al, 2010, Singh et al, 2010). Aluminium nanomaterials act as drug delivery systems, by encapsulating the drugs the drugs to increase solubility for evading clearance mechanisms and allowing the site-specific targeting of drugs to cells (Tyner et al, 2004).

Previous toxicological studies on nanomaterials were conducted on TiO_2 , CdO_2 , C_{60} , and carbon nanotubes only (Pan et al, 2010, Horváth et al, 2011). The toxicity of iron oxide nanoparticles (IONPs), although they are the only metal oxide nanoparticles approved for clinical use, has been investigated only in a small number of studies.

1.2.1 Iron and iron oxides in nature

Iron and its compounds are widespread in nature and readily synthesized in the laboratory. Iron compounds present in the hydrosphere, the lithosphere and (as pollutants) in the atmosphere. Iron is a biogenic element, present in all biota, but some iron compounds can cause harmful effects to humans, animals, and environment (Gurzau et al, 2003, Cornell and Schwertmann, 2003). In occupational exposure of humans, iron and iron oxides are known to produce benign siderosis – but iron oxides have been implicated also as a vehicle for transporting high concentrations of carcinogens and sulfur dioxide deep into the lungs, thereby enhancing the activity of these pollutants (Gurzau et al, 2003). Iron oxides also cause damage by staining materials. Analyses of urban air samples showed that the probable sources of iron compounds are the iron and steel industry (Gurzau et al, 2003) and urban transport

such as underground railways (Hurley et al, 2003, Dura and Szalay 2007). Tunnel dust – generated by interaction of brakes, wheels and rails – contains about 90% iron, 1–2% quartz and the remnants of other metals in the underground rail system (Hurley et al, 2003).

There exist 6 iron oxides composed of Fe and O: hematite (α -Fe₂O₃), magnetite (Fe₃O₄), maghemite (γ -Fe₂O₃), β -Fe₂O₃, ϵ -Fe₂O₃ and Wüstite (FeO). In most of these compounds, iron is in the trivalent state, but FeO and Fe₃O₄ contain Fe(II) (Cornell and Schwertmann, 2003).

Hematite, α -Fe₂O₃, is the oldest known Fe oxide mineral and is widespread in rocks and soils. It is extremely stable and is often the final stage of transformations of other iron oxides. The blood-red-coloured hematite is an important pigment and a valuable ore. Other names for hematite include iron(III)oxide, ferric oxide, red ochre and kidney ore.

Magnetite, Fe₃O₄, is a black, ferromagnetic mineral containing both Fe(II) and Fe(III). Magnetite is an important iron ore. Together with titanomagnetite, it is responsible for the magnetic properties of rocks. It is formed in various organisms in which it serves as an orientation aid. Other names for magnetite include black iron oxide, magnetic iron ore, iron(II,III)oxide and ferrous ferrite.

Maghemite, γ -Fe₂O₃, is a red-brown, ferromagnetic mineral isostructural with magnetite, but with cation deficient site. It occurs in soils as a weathering product of magnetite or as the product of heating of other Fe oxides, usually in the presence of organic matter (Cornell and Schwertmann, 2003).

1.2.2 Iron in the human body

The content of iron in the human body is regulated by a complex mechanism for maintaining homeostasis. During childhood, pregnancy or blood loss, the need for iron is increased and so is the absorption. Absorption occurs in two steps: absorption of ferrous ions from the intestinal lumen into the mucosal cells, and transfer from the mucosal cell to the plasma, where it is bound to transferrin for transfer to storage sites. Transferrin is a β 1-globulin and is produced in the liver. As the Fe²⁺ ion is released into plasma, it becomes oxidized by oxygen in the presence of ferroxidase I. There are 3–5 g of iron in the body, about two-thirds of which is bound to hemoglobin, 10% to myoglobin and iron-containing enzymes, and the remainder is bound to the iron storage proteins ferritin and hemosiderin. Exposure to iron induces synthesis of apoferritin, which then binds ferrous ions. The ferrous ion becomes oxidized,

probably by histidine and cysteine residues, and by carbonyl groups. Iron may be released slowly from ferritin by reducing agents such as ascorbic acid, cysteine, and reduced glutathione. Normally, excess ingested iron is excreted, but some remains within shed intestinal cells, in bile, in urine, and in even smaller amounts in sweat, nails, and hair. Total iron excretion is usually ~ 0.5 mg/day (Ádám et al, 1996).

With excess exposure to iron or iron overload, there may be a further increase in ferritin synthesis in hepatic parenchymal cells. In fact, the ability of the liver to synthesize ferritin exceeds the rate at which lysosomes can process iron for excretion. Lysosomes convert the protein from ferritin to hemosiderin, which then remains in situ. The formation of hemosiderin from ferritin is not well understood, but it seems to involve denaturation of the apoferritin molecule. With increasing iron loading, ferritin concentration appears to reach a maximum and a greater portion of iron is found in hemosiderin. Both ferritin and hemosiderin are, in fact, storage sites for intracellular metal and are protective in that they maintain intracellular iron in bound form. A portion of the iron taken up by cells of the reticuloendothelial system enters a labile iron pool available for erythropoiesis, and part becomes stored as ferritin (Ádám et al, 1996, Gurzau et al, 2003).

1.2.3 Iron oxid nanoparticles

The two most commonly studied iron oxides have been magnetite (Fe_3O_4) and maghemite ($\gamma\text{-Fe}_2\text{O}_3$) (Gupta and Gupta, 2005b). IONPs are found naturally in the environment as particulate matter in air pollution and in volcanic eruptions. Either Fe_3O_4 (magnetite) or $\gamma\text{-Fe}_2\text{O}_3$ (maghemite), particles can be generated as emissions from traffic, industry and power stations but can also be specifically synthesised chemically for a wide variety of applications (Karlsson et al, 2008, Hurley et al, 2003, Faraji et al, 2009). Various methods can be employed in their fabrication such as synthesis by water-in-oil microemulsion system, co-precipitation, reactions in constrained environments, polyol method, flow-injection synthesis and sonolysis (Faraji et al, 2009, Laurent et al, 2008, Fievet et al, 1989).

Magnetic behaviour is an important parameter in design and synthesising of superparamagnetic iron oxide NPs (SPIONs) in order to maximally facilitate their imaging and therapeutic efficacy as these applications require high magnetisation values. Although this can be accomplished by applying a maximum magnetic field acceptable under the clinical settings, the reaction conditions during the synthesis processes can be modulated to generate particle size with a large surface area, which in turn allows these particles to exhibit high magnetic susceptibility (Gould, 2006, Goya et al, 2003).

Suh et al (2009) summarized several results of research groups that have examined toxicology of iron oxides in recent years:

Type & size	Animal / cell type and Method	Result
Fe ₂ O ₃ NPs; 5; 12 nm	Rat pheochromocytoma cell line (PC12) Fluorescent live/dead cell staining	Exposure to 0.15-15mM NPs: dose-dependent diminishing ability of PC12 cells to differentiate in response to NGF
Fe ₂ O ₃ NPs; 5; 45 nm	Human aortic endothelial cells (HAECs) Measured protein levels of the inflammatory markers	NPs fail to provoke an inflammatory response in HAECs at any of the concentrations (0.001-50µg/ml) tested
Fe ₂ O ₃ NPs; 12–50 nm	Human mesothelioma (MSTO); Rodent fibroblast cell lines (3T3) MTT assay, total DNA measurement	Cytotoxic for MSTO cells for both MTT and DNA (1-30ppm for 3 days) Iron ion concentration coupled with nanoparticle uptake may be the cause of increased toxicity Non-cytotoxic for 3T3 cells (MTT and DNA)
Fe ₃ O ₄ NPs; 30; 47 nm	Rat liver derived cell line (BRL3A) MTT and LDH assays (24h)	No measurable toxic effect between 10-50 µg/ml Toxic at high conc. of 100-250 µg/ml
SPION (Ferumoxtran-10) 30 nm	Rats, rabbits, dogs and monkeys (lymph nodes) Pharmacokinetic, safety pharmacology; Single and repeated dose study; Reproduction toxicity; Genotoxicity toxicity	2, 13, 40, 126, 400 (mg Fe/kg) Toxic at high iron conc. with repeated injections Not mutagenic but teratogenic in rats and rabbits
SPION (AMI-25) 30 nm	rats, beagle dogs Acute toxicity: 28 mg Fe/kg or 168 mg Fe/kg Subacute toxicity: 0-14 mg Fe/kg Mutagenicity (Ames test): 0-2140 µmol Fe/kg	Acute toxicity: no adverse effects Subacute toxicity: all within normal ranges; no tissue damage Mutagenicity (Ames test): non toxic
Ferumoxides-poly-L-lysine (PLL) 38.8 kD	Human mesenchymal stem cell; Human cervical carcinoma cells (HeLa) 25 µg/ml per 5000 cells MTT assay Apoptosis assays ROS measurement	Long-term viability, growth rate, and apoptotic indices of the labeled cells were unaffected by the endosomal incorporation of SPION Nonsignificant transient increase in reactive oxygen species Had no short- or long-term toxic effects on tumor or mesenchymal stem cells

Table I Iron oxide nanotoxicology (based on Suh et al, 2009).

1.2.4 Biomedical applications of iron oxide nanoparticles

SPION have some unique physico-chemical features, such as nanometre sizes and a large surface area to mass ratio that also facilitate novel applications (Singh et al, 2010). Due to their magnetic properties SPIONs have been extensively used in a number of bioapplications including magnetic drug and gene delivery (Faraji et al, 2009, McBain et al, 2008), tissue repair, cell separation (Gupta and Gupta, 2005a), magnetic resonance imaging (MRI; Bulte et al, 2004, Schlorf et al, 2011) and magnetic fluid hyperthermia (Kumar et al, 2011). Antibody-targeted SPIONs can be used for diagnosis and targeted therapy of cancer (Vigor et al, 2010).

SPIONs have an MRI contrast enhancement potential (Bulte et al, 2004). Upon application of a magnetic field the magnetic moments within the SPIONs align in the direction of the field, this gives rise to a large net magnetic moment, in comparison, paramagnetic material exhibit only a small net magnetic moment (Goshima et al, 2004; Mornet et al, 2004). The large magnetic moment generated by SPIONs leads to a disturbance in the local magnetic field, causing a shortening of the hydrogen nuclei relaxation times. This shortening in proton relaxation times leads to a detectable change in the T2 MRI signal (Mornet et al, 2004).

Currently there are two FDA approved SPION contrast enhancement agents, Endorem® EU (Ferridex USA) and Resovist® (Schering AG), both used for liver and spleen imaging. Sinerem EU (Combindex USA) is another SPION contrast agent currently in phase III trial for application in lymph node imaging (Vigor et al, 2010).

With the possibility to convert dissipated magnetic energy into thermal energy, the application of magnetic materials for hyperthermia treatment of cancer was first proposed in 1957 (Gilchrist et al, 1957). Since then the approach evolved into a well-researched field due to the introduction of magnetic nanoparticles (MNPs). MNPs-based hyperthermia treatment has a number of advantages compared to conventional hyperthermia treatment. These are: 1) cancer cells absorb MNPs thereby increasing the effectiveness of hyperthermia by delivering therapeutic heat directly to them, 2) MNPs can be targeted by means of cancer-specific binding agents making the treatment much more selective and effective, 3) MNPs can also effectively cross blood-brain barrier and hence can be used for treating brain tumors (Kumar and Mohammad, 2011), 4) effective and externally stimulated heating can be delivered at cellular levels through alternating magnetic field (Ito et al, 2006), 5) with the possibility to obtain stable colloids using MNPs, they can be administered through a number of drug

delivery routes (Faraji et al, 2010), 6) MNPs used for hyperthermia are only few tens of nanometer in size and therefore, allows easy passage into several tumors whose pore sizes are in 380-780 nm range (Brigger et al, 2002), 7) compared to macroscopic implants, MNPs-based heat generation is much more efficient and homogeneous (Bahadur and Giri, 2003), 8) MNPs-based hyperthermia treatment may induce antitumoral immunity (Ito et al, 2005), and 9) last but most important aspect is that MNP-based hyperthermia can also be utilized for controlled delivery of drugs and the first such nanoconstruct for this purpose has been made using layer-by-layer self-assembly approach (Zonghuan et al, 2005). This additional feature opens up possibilities for the development of multifunctional and multi-therapeutic approaches for treating a number of diseases (Kumar and Mohammad, 2011).

Tumour cells have shown a greater sensitivity to heat treatments compared to healthy cells (Zee, 2002). This has led to the use of thermo-ablation and hyperthermic therapies in the clinic, often in combination with other treatments. The first clinical study of magnetic fluid hyperthermia by Johannsen et al (2005) showed that direct injection of 12.5 ml SPION suspension into the prostate at concentrations of 120 mg/ml was well tolerated.

Systemic application of SPIONs however, proves more difficult due to their rapid clearance from the blood by the RES and therefore, reducing the concentration of SPIONs reaching the target organ. To improve the systemic application of SPIONs functionalisation with a targeting moiety would be advantageous (Vigor, 2010).

1.3 Aims of the study

Both magnetite (Fe_3O_4) and maghemite ($\gamma\text{Fe}_2\text{O}_3$) iron oxides occur naturally (for example as nano-sized crystals in the earth's crust generated by various environmental sources such as volcanoes and fires) and artificially as engineered NPs which offer a high potential for several application. The major concern is the increased exposure (via different routes) level to humans and the ecosystem as more and more NPs are being manufactured to meet the demands of the rapidly proliferating field of nanomedicine (Borm et al, 2006). The dramatic growth and the therapeutic benefits that iron oxide nanoparticles have to offer, accompanies the risks and concerns associated with their exposure (Maynard et al, 2006). Therefore, there is a considerable need to evaluate of exact toxic effects of IONPs associated with their usage in a variety of applications.

This study focuses on one of the most widely used NPs in medical diagnostics, aiming to highlight the potential (and up to now not completely examined) adverse biological effects associated with IONPs. We know that *in vitro* cell cultures will not be able to replace animal experiment completely, on the other hand *in vivo* animal tests have disadvantages: the high costs, the ethical concerns and their questionable value presumably false hopes are raised regarding product safety on the basis of animal tests only. But by combining these in a complex experimental model, early detection of possible toxicological effects can be achieved, and new relationships between the primary outcomes can be revealed. Therefore the thesis presents both *in vivo* and *in vitro* tests for toxicological examination of IONPs.

The questions to be answered in this thesis were as follows:

- 1) Does intratracheal application of iron oxide nanoparticles cause any general toxic effect and general and or specific histopathological changes in rat organs?
- 2) Does it cause any specific toxic effect on rat respiratory system?
 - a) Does it change production of any immunoglobulin in the early stage of exposure in BAL and the whole blood?
 - b) Does it cause changes of some components of pulmonary redox system?
- 3) Does it cause any harmful effect in *in vitro* cell lines?
 - a) Does it cause any damage in the primary culture of rat lung cells and human A549 cell line?
 - b) If yes, is there any relationship between cell damage and production of pro-inflammatory proteins?
 - c) Does it induce cytotoxic effect in another mammalian cell line?
- 4) Can mutagenic activity be detected in bacterial cells exposed to iron oxide nanoparticles?

2 MATERIALS AND METHODS

2.1 Iron oxide nanoparticles

IONPs were obtained from Sigma-Aldrich Co. (Budapest, Hungary). The characteristics of IONPs as reported by the manufacturer are: iron(II,III)oxide nanopowder (Fe_3O_4), spherical, < 50nm particle size (transmission electron microscope, TEM), $\geq 98\%$ trace metals basis, BET (Brunauer, Emmett and Teller) surface area $> 60\text{m}^2/\text{g}$; iron(III)oxide nanopowder (Fe_2O_3), crystalline, < 50nm particle size (TEM), BET surface area: 50–245 m^2/g . The average particle size and shape of the nanoparticles were checked by transmission electron microscopy (Figure 1).

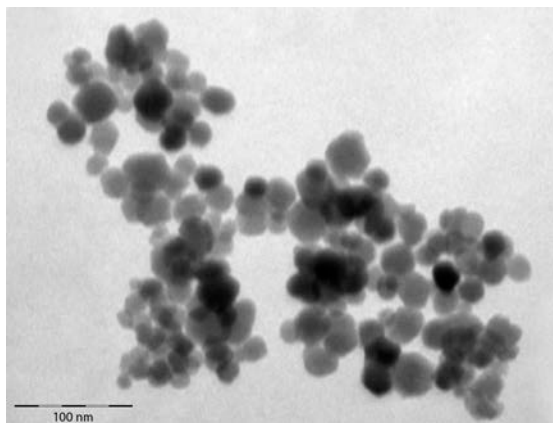


Figure 1 TEM image of size and morphology of IONPs. Scale bar: 100 nm.

2.2 *In vivo* experiments

Table 1 summarizes the *in vivo* and *in vitro* experiments iron oxide nanoparticles toxicology with focus on aims, methods and results.

2.2.1 Animals and treatment

In Experiment I adult male Wistar rats obtained from the breeding centre of University of Szeged were used (260 ± 10 g body weight at start, see Figure 2). In Experiment II and III adult male Sprague Dawley (SPRD) rats obtained from Charles-River (Isaszeg, Hungary) were used (210 ± 10 g body weight at start). The rats were housed in clean polypropylene cages and maintained in an air-conditioned conventional animal house at $22\pm 2^\circ\text{C}$, 50–70% relative humidity and 12h light/dark cycle. The animals were provided with commercial rat pellet and tap water ad libitum. After one week acclimatization, the rats were randomly divided into three (in Experiment II and III) or four groups (in Experiment I): untreated control, control, low dose and/or high dose IONPs (see Table 2). The rats were treated once during the experiments. In Experiment I each group contained 30 animals at start and 6 of the 30 rats per group were sacrificed after 1, 3, 7, 14 and 30 days respectively. In Experiment II each group contained 24 animals at start and 6 of the 24 rats per group were sacrificed after 1, 3, 7 and 14

EXPERIMENT		AIM	METHOD	RESULT
IN VIVO	I	general toxic effect: body and organ weight analyses	single intratracheal instillation 1, 5 mg/ml IONPs (Table 2)	significantly slowed body weight gain (Figure 2); weight of the lungs decreased (Table 3)
		histopathological examination: lungs, liver, kidneys, spleen	HE, Berlin blue, Giemsa, Gömöri's and van Gieson stains	no abnormalities in the exposed rats' organs except in the lungs (Figure 3)
	II	immunological examination: Ig level changes	single intratracheal instillation 1 mg/ml IONPs (Table 2)	IgA (blood): ↓; IgA (BAL): – IgG and IgM (blood): –
			blood and bronchoalveolar lavage samples	IgG and IgM (BAL): ↓ (Figure 4)
III	biochemical examination: effect of IONPs on pulmonary redox system	single intratracheal instillation 1 mg/ml IONPs (Table 2) homogenisation of the lungs	GSH and EC-SOD changes: –	
IN VITRO	IV	effect of IONPs on primary culture of rat lung cells and human A549 cell line	isolation of AM and PII from 6 SPRD rats; AM, PII and A549 cells (Figure 5); exposition to 1, 5, 10µg/ml IONPs; incubation: 24h	viability of each cell types: 92-94% IONPs caused the injury of cellmembranes; human cells were more sensitive (Figure 6)
			trypan blue (viability) test	
			lectin histochemistry assay	
	V	relationship between cell damage and proinflammatory proteins	isolation of AM and PII from 6 SPRD rats; AM, PII cells: exposition to 1, 5, 10µg/ml IONPs; incubation: 24h	viability of each cell types: 92-94% AM cells - MCP-1 (5 and 10µg/ml): ↑; AM cells - MIP-1α (10µg/ml): ↑ (Figure 7)
			trypan blue (viability) test	PII cells - MCP-1 (1, 5 and 10µg/ml): ↑;
			chemokine detection	PII cells - MIP-1α: – (Figure 8)
	VI	cytotoxic effect of IONPs	Vero cells: exposition to 78 - 10000 µg/ml IONPs; incubation: 4 and 24h	time- and concentration dependent cytotoxicity (Figure 9)
VII	genotoxic effect of IONPs	bacterial reverse mutation assay	no mutagenic effect (Figure 10-12)	
		4 <i>Salmonella typhimurium</i> and 1 <i>Escherichia coli</i> strains with and without metabolic activation exposition to 6.9 - 5000 µg/ml IONPs; incubation: ca. 60h		

Table 1 Summary of the experiments performed.

days respectively. In Experiment III each group contained 12 animals at start and 6 of the 12 rats per group were sacrificed after 7 and 30 days respectively.

For administration, the IONPs were suspended in physiological saline and instilled into the rats' trachea under halothane anaesthesia (Lèciva, Prague). An untreated control (UnC, neither anesthesia nor intratracheal instillation) and a vehicle control group (Con, anesthetized and vehicle treated) was used. Doses, group coding and treatment scheme are shown in Table 2. The instilled volume was 1 ml/kg body weight. Before and during instillation, the nanosuspension was repeatedly sonicated (Elmasonic E15H, Germany) to prevent aggregation and sedimentation.

Group*	Code	Number of animals in each <i>in vivo</i> experiment			Treatment and dose
		I	II	III	
Untreated control	UnC	30	24	12	—
Vehicle control	Con	30	24	12	0.9% physiology saline 1 ml/kg body weight
Low dose	LD	30	24	12	Fe(II,III)O nanosuspension, 1 mg/kg body weight; 1 ml/kg body weight
High dose	HD	30	—	—	Fe(II,III)O nanosuspension, 5 mg/kg body weight; 1 ml/kg body weight
Time of sacrifice; after <i>n</i> days of single intratracheal instillation in all groups		1, 3, 7, 14, 30	1, 3, 7, 14	7, 30	

Table 2 Treatment groups and the corresponding doses in *in vivo* experiments. *The groups started with 30/24/12 rats each; 6 rats per group were sacrificed after 1, 3, 7, 14, and/or 30 days, respectively.

The animal tests were done in adherence to the requirements by the Ethical Committee of Animals of the Institute and the University.

2.2.2 General toxicological and histopathological examination

In Experiment I (an *in vivo* experiment) body and organ weights were monitored, and histopathological analysis was undertaken. The rats' body weight was recorded before NP administration, and then every two days and once more on the day of sacrifice. In terminal halothane narcosis, the animal was exsanguinated by cutting the abdominal aorta and was dissected. The organ weight of the brain, liver, lungs, heart, kidneys, spleen, thymus and

adrenals was measured. From these data, relative weights were calculated by relating absolute organ weights to brain weight. Brain weight was used as reference (Schärer, 1977) because (in contrast to body weight) it was minimally affected by the treatment. Small tissue samples from the mentioned organs were fixed in 8% neutral buffered formalin, embedded into paraffin, sectioned for 5–6 µm thick, and stained with hematoxylin eosin, Berlin blue reaction, Giemsa, Gömöri's silver impregnation and elastic van Gieson stains using standard histopathological techniques. The sections were examined by light microscopy.

2.2.3 Immunological examination

In Experiment II the rats were anaesthetized and sacrificed after 1, 3, 7 and 14 days after exposure. Blood samples were taken from the abdominal aorta and bronchoalveolar lavage (BAL, see in vitro experiment) was carried out with physiological saline by adding phenyl-methylsulphonyl fluoride (PMSF, Sigma-Aldrich) as a protease inhibitor to the BAL. IgA, IgG, and IgM concentrations were determined by the conventional sandwich enzyme-linked immunosorbent assay (ELISA) method. Polyclonal antibodies were purchased from Serotec (Kidlington, Oxford, UK). Serum samples (five animals per group) were diluted 1:2000 and BAL samples 1:50. A twofold dilution of pooled normal rat serum was used as a standard. Microwell plates (Greiner) were incubated overnight with 100 µl per well of antibody solution at 4°C; anti-rat IgA (heavy-chain, MCA191), anti-rat IgG (heavy-chain, MCA194B) and anti-rat IgM (heavy-chain, MCA189) a carbonate-bicarbonate buffer (pH 9.5). The plates were washed again with PBS-T buffer (0.1% Tween 20 v/v) and then 100 µl dilute samples and standards were added in duplicate wells and incubated at 37°C for 1h. The plates were washed again with PBS-T and then 100 µl of corresponding peroxidase-labelled antibodies (dilution 1:1000 in PBS-T buffer) were added and maintained for 30 minutes at 37°C. After washing with PBS-T, 150 µl per well of substrate (TMB: 3,3',5,5'-tetramethylbenzidine liquid substrate supersensitive for ELISA, Sigma-Aldrich) was applied. The reaction was stopped with 50 µl of 2M sulphuric acid. Absorbance was measured at 450 and 620 nm.

2.2.4 Biochemical examination

In experiment III after 7 and 30 days of exposure the animals were sacrificed, as above. The lungs were frozen in liquid nitrogen and placed in a freezer (five animals per group, –80°C). Homogenisation of the lungs was performed on the same day as total glutathione (GSH) estimation. After homogenisation, samples were centrifuged at 10000 rpm for 30 minutes at 4°C. GSH was determined using the GSH reductase method (Anderson, 1985). Extracellular

Cu,Zn/superoxide dismutase (EC-SOD) was estimated with the use of a Radox kit (Radox Laboratories Ltd, UK). In this method xanthine and xanthine oxidase generate superoxide radicals, which react with 2-(4-iodophenyl)-3-(4-nitrophenol)-5-phenyltatrazolum chloride to form a red formazan dye. Activity was measured by the degree of inhibition at a wavelength of 412 nm (Fridovich, 1986; Meister and Anderson, 1983). All determinations were performed in duplicate. Protein was determined according to Lowry et al. (1951). The results were expressed in milliunits of activity per mg protein (SOD) or mM/mg protein (GSH).

2.3 *In vitro* experiments

Table 1 summarizes the *in vivo* and *in vitro* experiments iron oxide nanoparticles toxicology with focus on aims, methods and results.

2.3.1 Cell lines and cultures

Human lung adenocarcinoma cell line (A549) was obtained from the National Research Institute for Radiobiology and Radiohygiene (Budapest, Hungary). Vero cell line was obtained from the National Centre for Epidemiology (Budapest, Hungary). Cells were cultured in Dulbecco's modified eagle's medium (DMEM) (A549) or RPMI 1640 medium (Vero) containing 10% (v/v) heat-inactivated fetal bovine serum, 100 U/ml penicillin and 100 µg/ml streptomycin at 37°C in a humidified 5% CO₂ incubator, and passaged once every 2–3 days. Media, serum and antibiotics were obtained from Sigma-Aldrich Co. (Budapest, Hungary).

2.3.2 Bacterial strains and rat liver S9-based metabolic activation system

S. typhimurium TA98, TA100, TA1535, TA1537 and *E. coli* WP2uvrA strains were supplied by Xenometrix AG (Allschwil, Switzerland). The strain genotypes were confirmed by testing the presence of specific genetic markers and phenotypes in preliminary strain check assays. Permanent cultures were then prepared and frozen. The S9 metabolic activator was prepared right before use, by adding: phosphate buffer (0.2 M) 5 ml; S9 fraction 1 ml / 2 ml (10% / 20%); deionised water 3 ml; MgCl₂ 6H₂O (Reanal, Hungary) (8 mM) 1.3 mg; KCl (Reanal) (33 mM) 24.6 mg; glucose-6-phosphate (Sigma) (5 mM) 14.1 mg and NADP (Reanal) (4 mM) 3.7 mg. The S9 mixture was kept on ice during testing. S9 fraction (i.e. the liver postmitochondrial supernatant of rats treated with the mixture phenobarbital/β-naphthoflavone (PB/NF) to induce the hepatic microsomal enzymes) was obtained from the Laboratory of Environmental Mutagenesis (National Institute of Environmental Health,

Budapest). Protein concentrations of the S9 fractions were determined according to [Lowry et al. \(1951\)](#) using bovine serum albumin as standard.

2.3.3 Lung cells and exposure

Alveolar macrophages (AM) and type II pneumocytes (PII) were isolated from male SPRD rats (Charles-River) weighing 190 ± 10 g (Experiment IV and V). The animals were maintained in the same way as in *in vivo* experiments. Under intraperitoneal sodium pentobarbitone anaesthesia (35 mg/kg nembutal, Sanofi-Aventis, Budapest) the animals were exsanguinated by cutting the abdominal aorta. The lungs were perfused through the pulmonary artery with 0.9% saline, then the lungs and trachea were removed from the thoracic cavity and 8–9 ml of 0.9% saline was instilled five times via a tracheal cannula (bronchoalveolar lavage, BAL). The AM were collected from the BAL in each *in vitro* experiment. The lungs were digested by protease solutions, then PII were obtained as described previously ([Richards et al., 1987](#)). Viability was examined by the trypan blue exclusion test. In control and treated PII the activity of alkaline phosphatase (AP) was assessed to check the purity of the cell culture. The cells (AM, PII and human A549) were plated on 24-well plates (Gibco, 10^6 cells per ml) and placed in a humidified 5% CO₂ incubator for 24h at 37°C. Dulbecco's Modified Eagle's medium (DMEM, Sigma) was changed from cells after 24h. DMEM contained IONPs at concentrations 1, 5 and 10 µg/ml were exposed for 24h. Control cells were exposed only to the medium. Viability was determined by the trypan blue exclusion test.

2.3.4 Lectin histochemistry assay

In Experiment IV animal AM, PII and human A549 lung cells were examined lectin histochemistry which is suitable for detection of oligosaccharide molecules bound to protein molecules in the cell membranes ([Sharon and Lis, 1989](#), [Tátrai et al., 1994](#)). Lung cells were exposed to IONPs at doses 1, 5, and 10µg/ml. After 24h incubation the cells were fixed in 4% neutral buffered formalin (pH 7.4) for 10 min at RT. After being washed in phosphate buffer saline (PBS, pH 7.4) cells were incubated with biotinylated lectins (20 µg/ml) for 20 min at RT. *Maclura pomifera* agglutinin (MPA, Sigma) can bind specifically the terminal α-D-galactose/galactosamine in the membranes of PII. *Bandeiraea simplicifolia* agglutinin (BSA, Sigma) can bind the terminal N-acetyl-α-D-galactosamine sequences in the membrane of AM. *Soybean* agglutinin (SBA, Sigma) can bind the terminal N-acetyl-α-D-galactosamine sequences in the membrane of A549. After being rinsed in PBS, the cells were incubated with streptavidin-biotin-peroxidase complex (Sigma) 1:200 for 30 min at RT. Finally, they were

treated with a 3-3'-diaminobenzidine-4HCl(DAB)-H₂O₂ solution. For confirmation of the specificity of lectin staining, the cells were preincubated with appropriate hapten sugars (0.1M). Lectin binding was completely blocked or significantly weakened by hapten treatment.

2.3.5 Chemokine detection

In Experiment V the primary culture of rat AM and PII lung cells were exposed to IONPs at doses 1, 5, and 10 µg/ml. After 24h incubation the supernatants of the cells were collected. The monoclonal antibody-based sandwich ELISA was used to measure macrophage chemoattractant protein -1 (MCP-1) and macrophage inhibitory protein -1α (MIP-1α) levels in the supernatants (cell number 10⁶ /ml). Optical density (OD) was measured at 405 nm wavelength using multiscan ELISA reader. Concentration of the samples was calculated using the calibration curve generated by software (Ascent).

Detection of MCP-1. Two different epitopes of MCP-1 paired monoclonal antibodies were used (PharMingen, USA). Purified mouse anti-rat MCP-1 monoclonal antibody was used as a capture, and a biotinylated antibody for the detection of MCP-1 bound by the capture antibody. Recombinant rat MCP-1 protein (recMCP-1, PharMingen) was applied as a standard. Optimal dilutions of capture and biotin-labelled antibodies were titrated to obtain a linear standard curve. Capture antibody was adsorbed to the wells of high binding capacity microwell plates (Greiner, Germany) at a concentration of 4µg/ml in 0.05M carbonate buffer (pH 9.5). Dilution series of recMCP-1 standard was prepared in PBS buffer containing 0.1% Tween 20 in 0.01–10 µg/ml concentrations. Samples were diluted in PBS-Tween 20 in ratios 1:5, 1:10 and 1:20, respectively, depending on the concentration of the samples tested. 100-100 µl of standards and samples were added simultaneously to antibody coated wells and were incubated for 1h at RT. The samples were discarded and the wells were washed three times with PBS-Tween 20. Then 100-100 µl PBS was added to biotin labelled antibody, diluted to 0.5 µg/ml and incubated for 45min at RT. The plates were washed as above, then incubated for 15 min at RT with peroxidase labelled avidin conjugate (Dako, Denmark) diluted to 1:5000 for 15 min at RT. After the wells were washed four times, the colours were developed with 100 µl substrate solution containing 0.5 mg/ml tetramethyl-benzidine (TMB, Sigma), 0.03% H₂O₂ in phosphate-citric acid buffer. The reactions were stopped by 0.5M H₂SO₄ and OD were measured.

Detection of MIP-1 α . Anti-rat MIP-1 α (AAR30), recombinant anti-rat MIP-1 α (PRP22), and biotinylated MIP-1 α (AAR30B) were purchased from AbD Serotec. Optimal working dilution of biotinylated antibody was determined by checker board titration. Unlabelled MIP-1 α was used as a capture of antibody in a sandwich ELISA applied for the detection of MIP-1 α protein in cell culture supernatant. Recombinant protein was used to construct the calibration curve. The wells of microtiter plates were coated with the capture antibody at 4 mg/ml concentration in carbonate buffer. Samples diluted 1:4 and 1:10 in PBS-Tween 20 buffer and dilutions of standard protein were dispensed into the antibody coated wells. After 1h incubation at RT, the samples were discarded and the plates were washed with PBS. Biotin labelled antibody in 2 μ g/ml dilution was added and incubated for 1h at RT. The plates were washed with PBS buffer, then peroxidase labelled avidin conjugate (Dako, Denmark) diluted to 1:5000 was added for 15 min at RT. Colours were developed by substrate solution as described above.

2.3.6 Cytotoxicity assay

In vitro cytotoxic studies of NPs use different cell line, incubation time and colorimetric assays. As is clear from the literature, for NPs, the biological effects involve interaction with cellular components such as the plasma membrane or genetic materials (Arora et al, 2012). It is important to perform this assay for each NPs type because of their unique biological response.

In Experiment VI, Vero cells were grown in 96-well plates (3000 cells/well) until subconfluent. IONPs were then added to the cells at 78, 156, 313, 625, 1250, 2500, 5000 and 10000 μ g/ml concentration, and incubated for 4 and 24 hours. After incubation, the medium was discarded and 90 μ l fresh medium per well was added to the cells. 10 μ l 3-(4,5-dimethylthiazol-2-yl)-2,5-diphenyl-tetrazolium bromide (MTT, Sigma) reagent (5 mg/ml stock) was then added per well and the plate was incubated for 4 or 24 hours. After incubation, the medium was discarded from the wells and 200 μ l methanol (Merck, Hungary) was added to solubilize the formazan crystals formed. Reduction of MTT was quantified by OD at a measurement wavelength of 570 nm and a reference wavelength of 630 nm, using absorbance microplate reader (EL_x808TM; Bio-Tek, USA). Percentage viability of the cells was calculated as the ratio of mean absorbance of triplicate readings of sample wells (I_{sample}) compared to the mean absorbance of control wells (I_{control}): Cell viability (%) = ($I_{\text{sample}}/I_{\text{control}}$) \times 100.

2.3.7 Bacterial reverse mutation assay

Ames test (or bacterial reverse mutation assay) is a widely used *in vitro* assay for assess the genotoxic potential of chemicals and pharmaceuticals. The test employs histidine dependent mutant (*Salmonella typhimurium*) and tryptophan dependent (*Escherichia coli*) strains. In a preliminary experiment we assessed the “solubility” (more precisely, the ability to form fine suspension) of IONPs in the final treatment mixture to find the highest concentration to be used in the following assays. Insolubility was defined as the formation of a precipitate of the substance in the final mixture under the test conditions and evident to unaided eye (OECD, 1997). IONPs gave a precipitate at concentrations higher than 100 mg/ml (corresponding to 5 mg/plate), thus this concentration was selected as the maximum one to be tested. Starting from 5 mg/plate, serial dilutions were prepared by using a dilution factor of about 1:3.

In each test within Experiment VII, DMSO was used as a negative control. Various diagnostic mutagens: SAZ (1-2 µg/plate) for *S. typhimurium* TA1535 and TA100 without S9 mixture, NPDA (4 µg/plate) for *S. typhimurium* TA98 without S9 mixture, 9AAC (1 µg/plate) for *S. typhimurium* TA1537 without S9 mixture, MMS (1 µl/plate) for *E. coli* WP2uvrA as well as 2AA (1-2 µg/plate) for all *S. typhimurium* strains and 2AA (25 µg/plate) *E. coli* WP2uvrA strain with S9 mixture were included as positive controls. Toxicity of the test materials was evaluated as reduction in the number of revertant colonies and as change in the auxotrophic background growth (lawn) in comparison with control plates (Maron and Ames, 1983). A positive response in the test was defined as an increase (at least twofold above the control) in histidine- or tryptophan-independent revertant colonies in every strain (Ames et al., 1975).

2.4 Statistical analysis

All values were expressed as Mean±S.D. From the general toxicological data, group means (±SD) were calculated. All data were tested for significance with one-way analysis of variance (ANOVA), and significant difference between the groups was tested using a two-way paired Student's *t*-test, the MTT analyses were performed using Student's *t*-test for unpaired data. *P* values < 0.05 were considered statistically significant. The results of immunoglobulins were calculated on the basis of Bazin's results (Bazin et al., 1974). Ames test data were processed using standard statistical software COLONY (Version 2.3, York Electronic Research, Huntington, York, England) with recommendation of UKEMS (U.K. Environmental Mutagen Society) (Kirkland, 1994).

3 RESULTS

3.1 *In vivo* experiments

3.1.1 General toxicology and histopathology

Intratracheal instillation of IONPs (LD and HD) caused a significantly slowed body weight gain compared to UnC and Con groups from the first week on. UnC rats had normal weight gain during the treatment period and the weight gain in the Con group was similarly constant, although somewhat slower, but body weight gain was in both treated groups (i.e. LD and HD) significantly reduced throughout the whole post-administration period (Figure 2). Among the relative organ weights (Table 3), weight of the lungs decreased significantly with increasing dose and time (from the 7th day in HD, and the 14th day in LD). It is noteworthy that physiological saline instillation alone (group Con) had minimal effect on the lung weight. By the first week, significant decrease of the liver and kidney relative weight developed also but disappeared later. Apart from the lungs no significant changes could be observed in other organs by the fourth week.

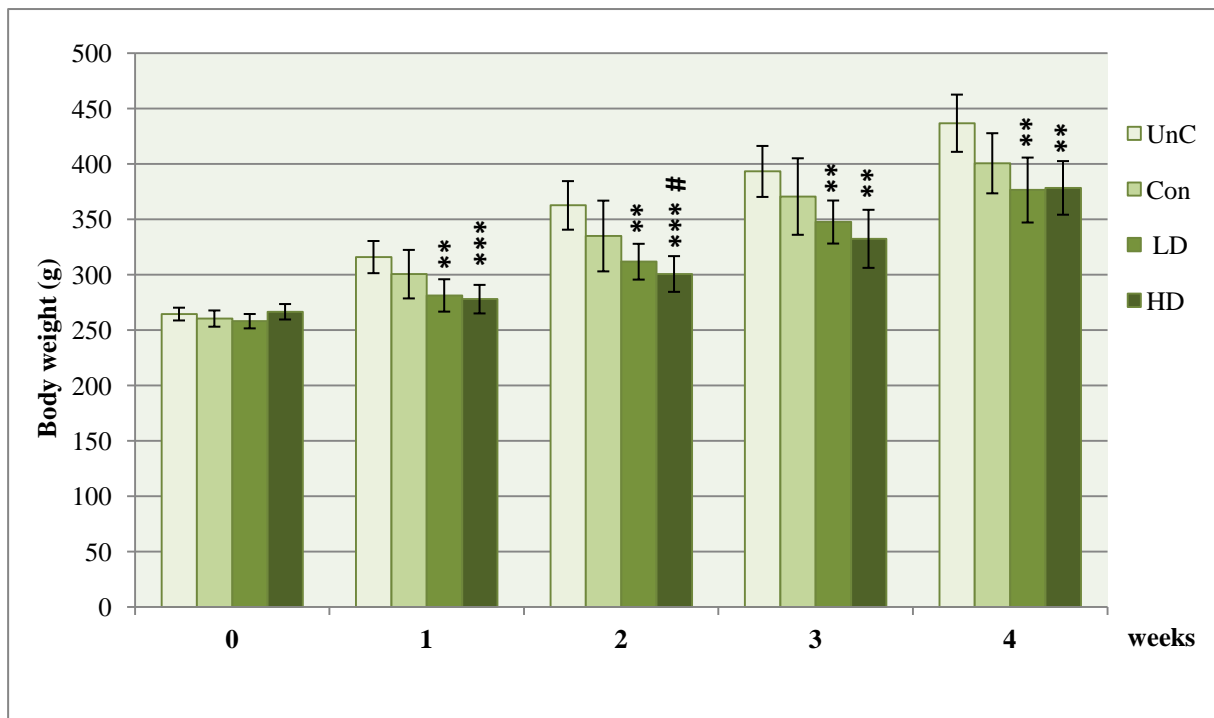


Figure 2 Body weight gain during the four weeks following single intratracheal administration of IONPs. Abscissa, weeks after treatment; ordinate, body weight (Mean \pm SD). Significance indicated by: **, *** $p < 0.01$; 0.001 vs. UnC; # $p < 0.05$ vs. Con.

Groups	UnC	Con	LD	HD
Relative organ weights, 7 days				
Lung	1.394±0.150	1.141±0.168	1.149±0.160	1.116±0.145*
Liver	8.841±0.555	7.773±0.807	7.339±0.519**	6.408±0.709**#
Kidney	1.682±0.081	1,408±0,138*	1.334±0.079***	1.205±0.134***#
Heart	0.476±0.013	0.549±0.086	0.552±0.079	0.464±0.051
Spleen	0.553±0.047	0.439±0.051*	0.445±0.081	0.427±0.090
Thymus	0.288±0.049	0.299±0.048	0.282±0.029	0.323±0.090
Relative organ weights, 14 days				
Lung	1.498±0.135	1,214±0,184	1.188±0.054**	1.105±0.119**
Liver	7.911±0.679	7.476±0.593	7.355±0.497	7.876±0.866
Kidney	1.444±0.040	1.356±0.094	1.467±0.040#	1.350±0.108
Heart	0.517±0.041	0.519±0.030	0.509±0.015	0.535±0.047
Spleen	0.442±0.051	0.439±0.057	0.424±0.051	0.429±0.021
Thymus	0.288±0.044	0.300±0.086	0.264±0.021	0.278±0.048
Relative organ weights, 30 days				
Lung	1.322±0.109	1,113±0,148	1.066±0.124*	1.140±0.119
Liver	7.875±0.662	7.098±0.689	7.000±0.586	7.404±0.626
Kidney	1.489±0.090	1.329±0.161	1.238±0.144*	1.463±0.123
Heart	0.527±0.049	0.515±0.019	0.481±0.075	0.543±0.028
Spleen	0.456±0.049	0.412±0.088	0.353±0.042*	0.386±0.052
Thymus	0.286±0.053	0.250±0.076	0.254±0.057	0.222±0.048

Table 3 Relative organ weights (Mean±SD, n=6 per group; related to brain weight); 7, 14, and 30 days after single exposure to IONPs. Significance: *, **, *** p < 0.05; 0.01; 0.001 vs. UnC; # p < 0.05 vs. Con. For group codes, see Table 2.

Pathological examination revealed no abnormalities in the exposed rats' organs (regional lymph nodes and internal organs compared to UnC or Con) except in the lungs. Within the alveoli and the lumina of capillaries IONPs could be detected by Berlin blue reaction (see Figure 3A; black arrows). In the treated rats' lungs, the interstitium was widened and infiltrated with lymphocytes, macrophages and plasma cells. After this focal, interstitial inflammation, a weak pulmonary fibrosis developed by the end of the one-month period (see Figure 3B; black arrows). In the interalveolar septa the amount of collagen fibres increased moderately (see Figure 3C; red arrows). The degree of pulmonary fibrosis and the collagen fibre growth were higher in the HD than in the LD rats (based on the evaluated sections).

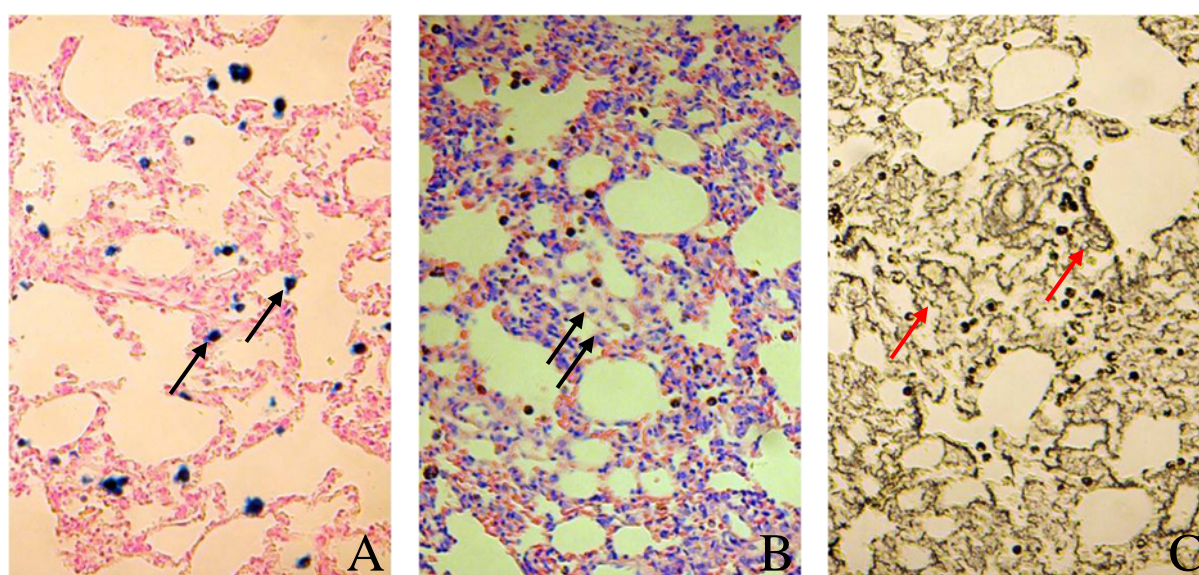


Figure 3 Lung tissue response in a rat exposed to high dose IONPs. The lung displays abnormal architecture compared to untreated and vehicle controls 30 days after instillation of NPs. (A) Berlin blue reaction, magnification x 280; (B) Giemsa staining, magnification x 320; (C) Gömöri's silver impregnation, magnification x 320.

3.1.2 Immunology

The *in vivo* immunological studies in Experiment II revealed that low dose IONPs decreased the IgA level in the blood (Figure 4A) but not in BAL (not shown). IgG and IgM (immunoglobulins of peripheral airways) showed significant decrease in BAL (Figure 4B and 4C) whereas they did not alter in the blood (not shown).

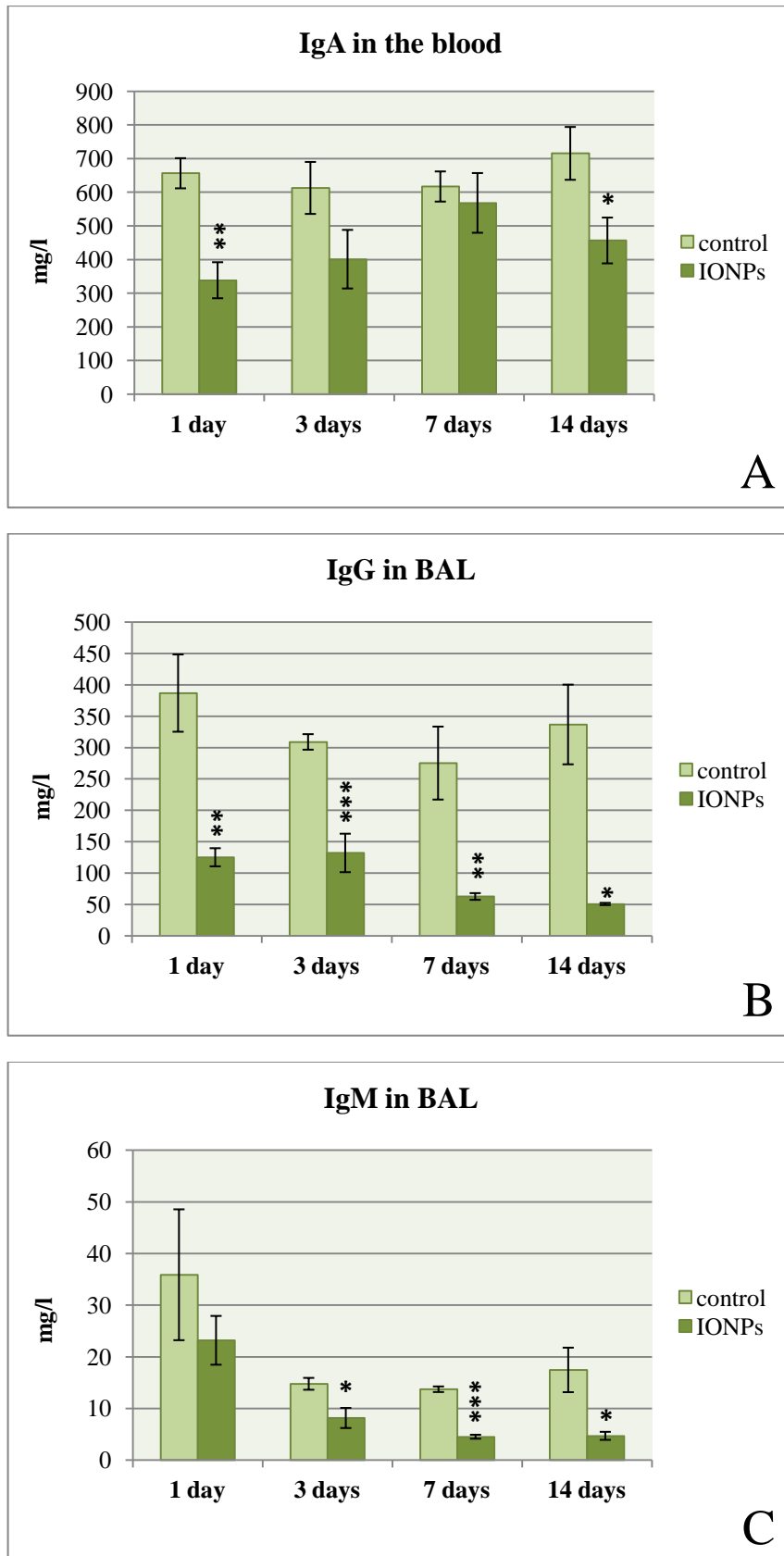


Figure 4 IgA levels (A) in the whole blood; IgG (B) and IgM (C) levels in BAL at different times after treatment. Abscissa, days after treatment; ordinate, immunoglobulin level; n=5 (Mean \pm SD). Significance: *,**,*** p < 0.05; 0.01; 0.001 vs. control.

3.1.3 Biochemistry

In this *in vivo* biochemical examination (Experiment III) GSH and EC-SOD were estimated. At 7 and 30 days after the exposure by IONPs neither GSH content nor EC-SOD activity could be measured (not shown).

3.2 *In vitro* experiments

3.2.1 Lectin histochemistry

These *in vitro* lectin histochemistry studies were performed in Experiment IV. After the trypan blue exclusion test indicated that viability of each cell type was 92-94% we examined the effects of IONPs on animal (AM, PII) and human lung (A549) cells by lectin histochemistry. Membranes of control (AM, PII and A549) cells were normal, and showed intact and regular staining (Figure 5, black arrows). At 1 and 5 $\mu\text{g/ml}$ concentrations of IONPs, the membranes of PII and AM cells proved to be intact similarly to control, while A549 cells (being more sensitive) showed incomplete membranes already at 1 $\mu\text{g/ml}$ concentration. At 10 $\mu\text{g/ml}$ concentration the membranes of both animal and human lung cells became irregular and lost continuity, finally the cells were fragmented indicating that IONPs caused injury of cellmembranes (Figure 6).

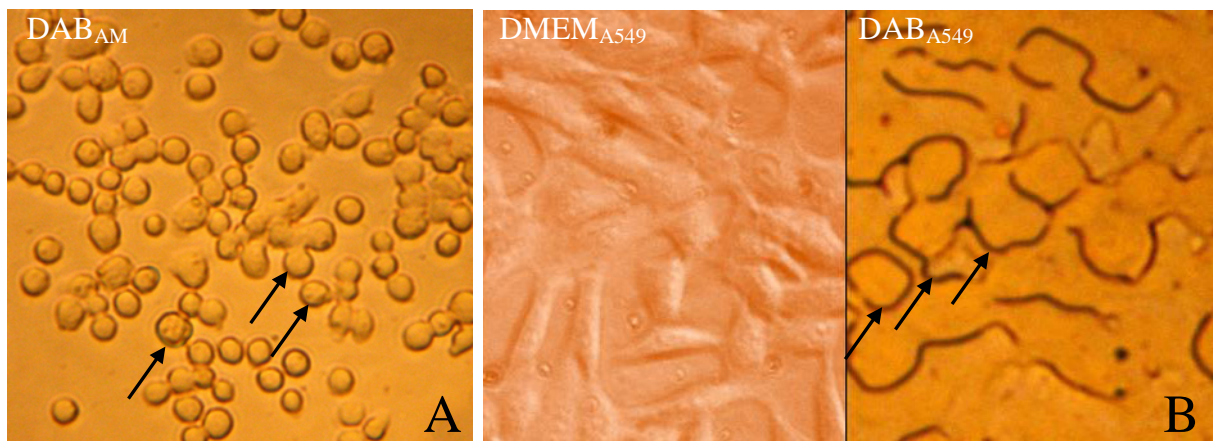


Figure 5 Uninjured cell membranes of (A) untreated alveolar macrophages (Control AM) and (B) human A549 cells (Control A549). Magnification x 25 (AM); x 40 (A549).

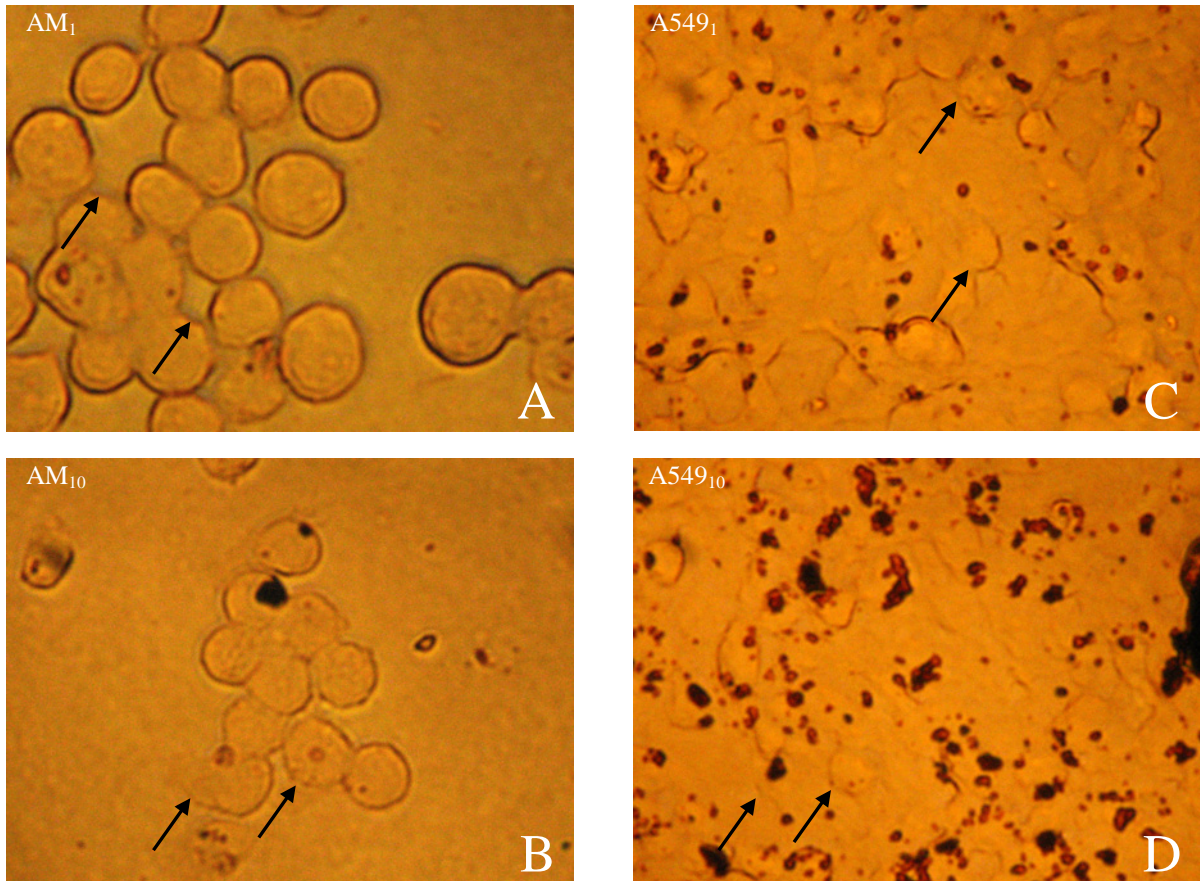


Figure 6 (A) Alveolar macrophages and (B) human A549 cells after 24 hours IONPs exposure at 1 µg/ml concentration. (C) Alveolar macrophages and (D) human A549 cells after 24 hours IONPs exposure at 10 µg/ml concentration. Black arrowheads show injury of cell membranes. Magnification x 40 in every case.

3.2.2 Chemokine detection

The *in vitro* experiments of chemokine detection were performed in Experiment V. In this tests, after 1, 5, and 10 µg/ml IONPs exposition, expression of the chemokines, macrophage chemoattractant protein -1 (MCP-1) and macrophage inhibitory protein -1α (MIP-1α) were determined. IONPs significantly increased the expression of MCP-1 and MIP-1α in AM (Figure 7). In PII cells, production of MCP-1 significantly increased while MIP-1α significantly decreased (Figure 8).

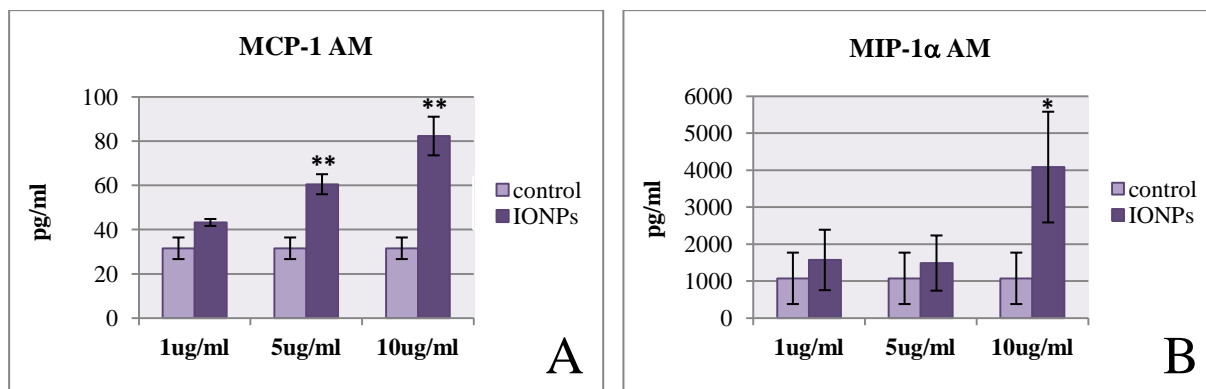


Figure 7 Primary culture of alveolar macrophages (AM) after treatment with 1, 5 and 10 µg/ml of IONPs. (A) MCP-1 and (B): MIP-1α production; n=5 (Mean ± SD). Significance: *, **, *** p < 0.05; 0.01; 0.001 vs. control.

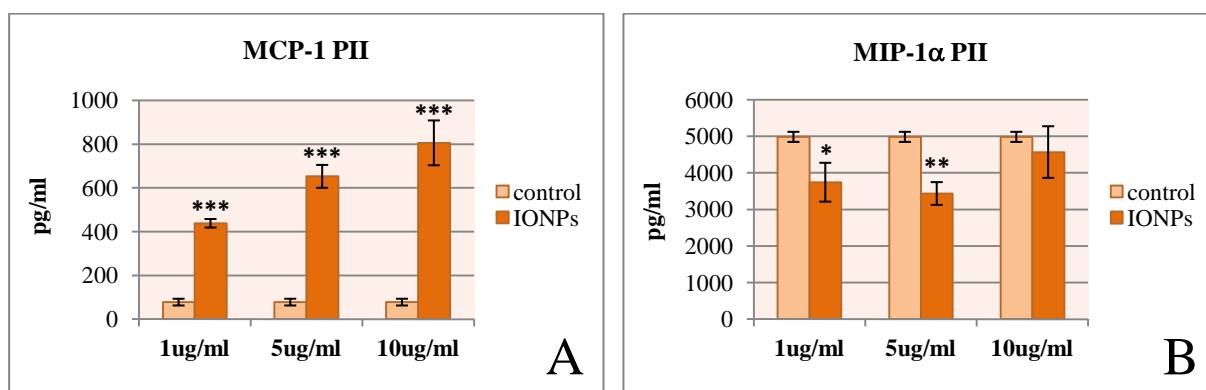


Figure 8 Primary culture of type II pneumocytes (PII) after treatment with 1, 5 and 10 µg/ml of IONPs. (A) MCP-1 and (B): MIP-1α production; n=5 (Mean ± SD). Significance: *, **, *** p < 0.05; 0.01; 0.001 vs. control.

3.2.3 Cytotoxicity

In Experiment VI *in vitro* cytotoxicity assay demonstrated that IONPs induced time- and concentration dependent cell loss in 24 hours. Cell viability changed from ca. 100% to approximately 12.8% with IONP concentrations increasing from 78 µg/ml to 10000 µg/ml. After only 4 hours incubation with the same concentrations of NPs, cell viability was similar to negative control (RPMI 1640 medium) (Figure 9). These results showed that IONPs had moderate cytotoxic effect.

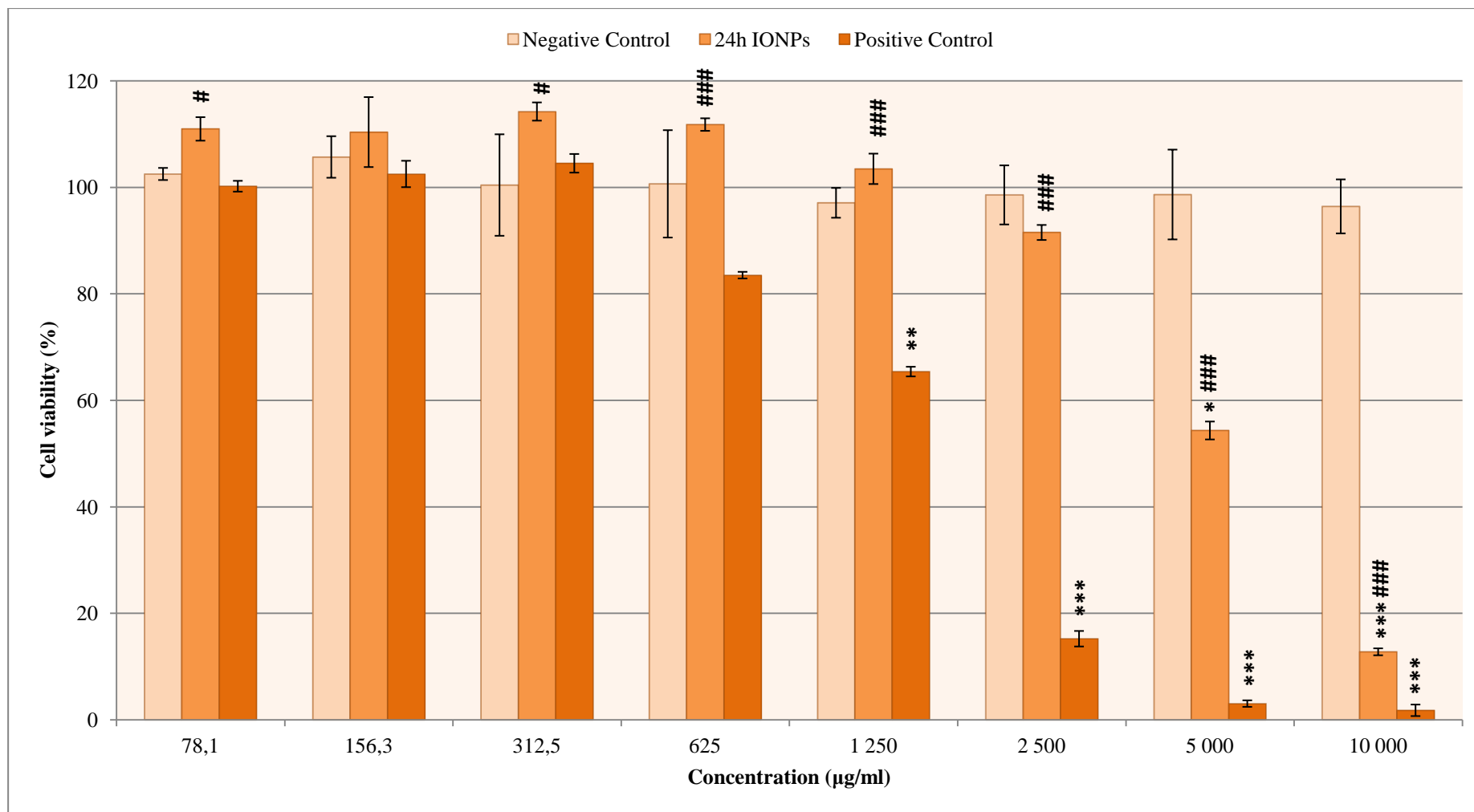


Figure 9 The effects of IONPs on cell viability of Vero cells as determined by cytotoxicity assay (Mean ± SD). Significance: *, **, *** p < 0.05; 0.01; 0.001 vs. Medium (as Negative Control); #, ##, ### p < 0.05; 0.01; 0.001 vs. Positive Control.

3.2.4 Genotoxicity

In *in vitro* Ames test (Experiment VII) a total of seven concentrations of IONPs (6.9-5000 $\mu\text{g}/\text{plate}$) were tested. The average number of revertant colonies and change in the background growth was similar in the IONP-treated groups and the negative control. None of the revertant rates was greater than or equal to the twofold of the negative controls, and no concentration-dependent increase was observed. In the negative control group of each tester strain, the average number of revertant colonies was within the range of the historical control data of our laboratory. The results were identical with and without metabolic activation. (Results are shown only in case of TA100 strain Figures 10, 11 and 12). The positive controls showed significant mutagenicity. These results demonstrated that IONPs are not mutagenic to the bacterial strains *Salmonella typhimurium* TA100, TA1535, TA98, TA1537 and *Escherichia coli* WP2uvrA.

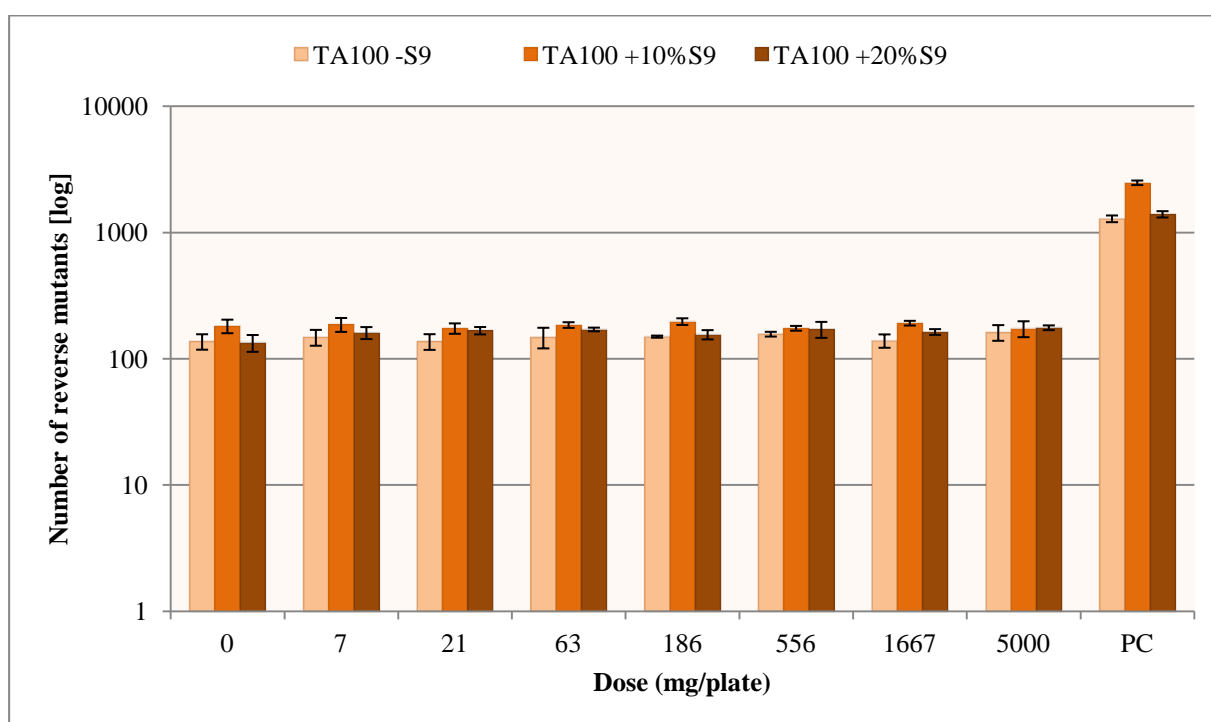


Figure 10 Mutagenic activity of IONPs in *S. typhimurium* TA100 with and without of S9 metabolic activation (Mean \pm SD; Negative Control (0): DMSO; Positive Control (PC): SAZ without S9 and 2AA with S9).

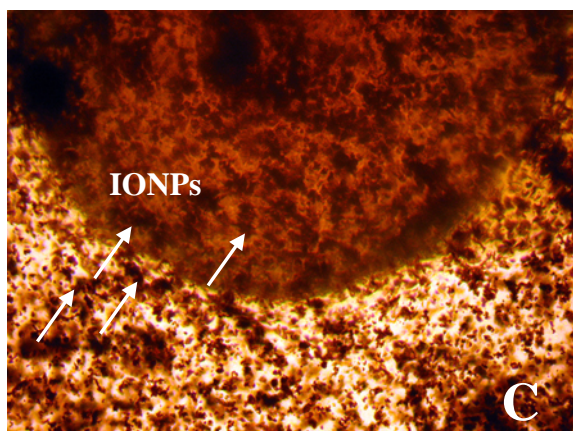
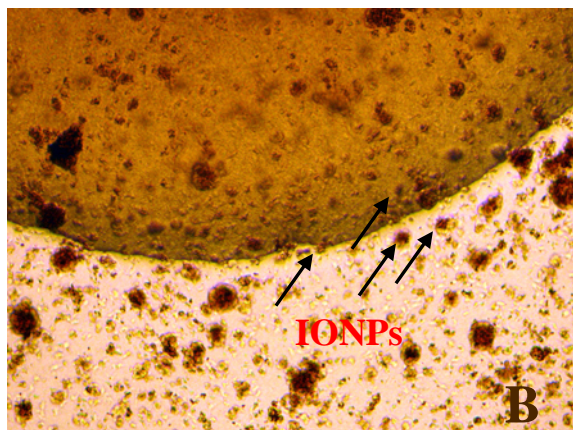
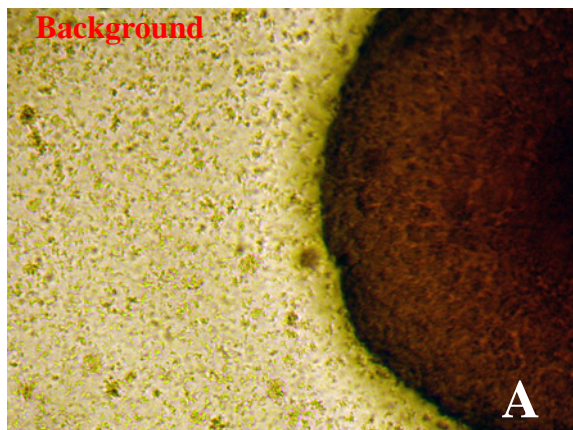


Figure 11 Light microscopy images of TA100 exposed to IONPs (without S9 metabolic activation)
 (A) 7 µg/plate;
 (B) 556 µg/plate;
 (C) 5000 µg/plate
 (Magnification x 50).

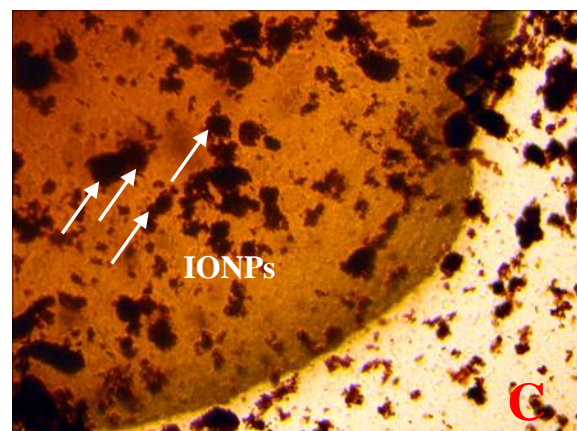
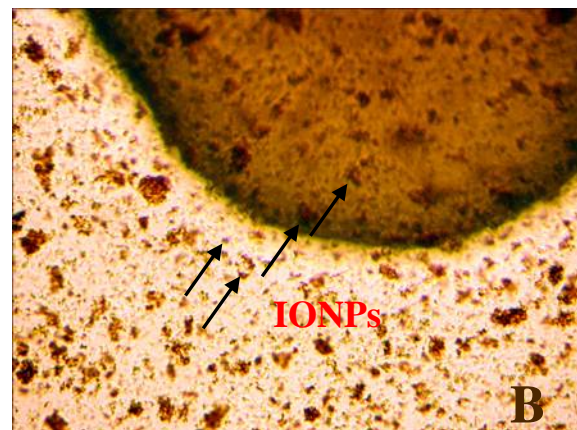
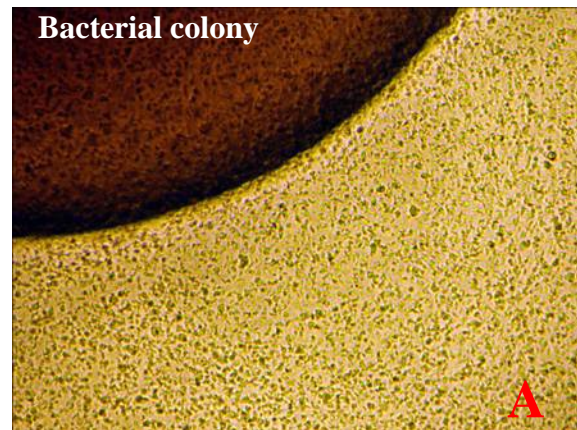


Figure 12 Light microscopy images of TA100 exposed to IONPs (+10% S9 system)
 (A) 7 µg/plate;
 (B) 556 µg/plate;
 (C) 5000 µg/plate
 (Magnification x 50).

Table 1 summarizes the *in vivo* and *in vitro* experiments iron oxide nanoparticles toxicology with focus on aims, methods and results (see page 13).

4 DISCUSSION AND CONCLUSION

In this study we applied a range of *in vivo* and *in vitro* tests to assess the possible toxic behaviour of iron oxide nanoparticles. Although predominantly magnetic (magnetite, Fe_3O_4 ; and maghemite, $\gamma\text{-Fe}_2\text{O}_3$) nanoparticles are the nanomaterials that have been approved for clinical use to date (Gould, 2006), studies on *in vivo* effects of IONPs are still scarce, and there has been some discrepancy in the literature about the adequacy of *in vivo* vs. *in vitro* methods for the toxicological assessment of NPs and the interpretation of the results. *In vitro* assays may seem preferable, being simpler, faster and devoid of ethical problems as opposed to *in vivo* studies (Sayes et al, 2007) – the correspondence between *in vitro* and *in vivo* results is, however, questionable (Mahmoudi et al, 2010).

The first question was whether intratracheal application of IONPs caused any general toxic effect and histopathological changes in animal test. The effect on body weight and the transient changes in the liver and kidney of the LD and HD rats indicated systemic action, which is in line with the observation of the presence of IONPs in the lumen of alveolar capillaries. The responsible mechanism is probably oxidative stress (even if neither GSH content nor EC-SOD activity could be measured in our experiment), the negative effect of which on body weight has been described after toxic exposure (Aoki et al, 2002) and in a chronic stress model (Rezin et al, 2008).

In the lungs of the treated rats, on the one hand after an interstitial inflammation a weak pulmonary fibrosis was observed and on the other hand there was a collagen fibre growth. In the rat model, lung exposures to nanoparticles typically produce greater adverse inflammatory and fibrotic responses than larger-sized particles of similar or identical composition at equivalent doses/mass concentrations (Warheit et al, 2008), and this holds true for respirable (as opposed to nano-sized) iron oxide dust too (Parkes, 1982). This fact and our histopathological results underline the importance and necessity of further *in vivo* toxicological experiments with IONPs, even if inhalation is a less likely way of purposeful application of IONPs to humans.

According to our second *in vivo* experiment, the lungs of the treated animals reacted independently of the general immune response: IgA level did not decrease in BAL but it decreased in the whole blood. IgM and IgG levels decreased in BAL whereas they did not change in the whole blood. The decrease in IgG and IgM levels confirmed the involvement of

peripheral airways in the pathological process, in the development of chronic interstitial inflammation.

The respiratory system represents a unique target for the potential toxicity of NPs. With the wide-spread environmental occurrence of NPs including iron, inhaled NPs are increasingly being recognised as a potential health risk (Oberdörster et al, 2005). Therefore, we have studied the impact of IONPs on human lung epithelial A549 cells, animal alveolar macrophages and pneumocytes type II in *in vitro* experiments. A549 is a model cell line for lung exposure (Ahamed, 2011).

The damage of the membranes of alveolar macrophages, pneumocytes type II and A549 cells pointed out the toxicity of IONPs. Application of these NPs caused permanent injury to the cell membranes, with disturbance of the structural oligosaccharide components in the cell membranes. Human A549 cells were more sensitive than animal cells, their membranes already were incomplete at low concentration.

Pneumocytes are extremely sensitive to different non-specific noxious agents. The completeness of cells is a precondition for the integrity of the lungs owing to the inhibition of clonal expansion of lymphocytes (Paine et al, 1993). Moreover, these cells normally release inhibitory mediators and alter fibroblast activation (Haschek et al, 1979). The pathological alterations of the alveolar epithelium may have an important role in the initiation and maintenance of inflammatory processes in the lungs. The alveolar epithelial cells produce a number of molecules through which they may regulate inflammatory and immune responses in the alveolar microenvironment. An important mechanism by which alveolar epithelial cells might regulate the inflammatory milieu of the alveolar space takes place through the production of chemokines. MCP-1 and MIP-1 α have chemotactic effect on the activation of monocytes or AM. Alveolar epithelial cells may control the local concentration and state of activation of alveolar macrophages and thus contribute to the initiation or maintenance of beneficial or harmful inflammatory processes within the lungs (Paine et al, 1993; Kovacs et al, 1994; Smith et al, 1995; Brieland et al, 1995).

On the basis of these results it may be stated that IONPs owing to particle size and huge surface induced the injury of membranes of AM, PII cells as well as A549, which led to release of chemokines and mild inflammatory response with fibrosis accompanied by immunosuppression.

According to cytotoxicity test IONPs caused moderate, time and concentration-dependent, cytotoxic effect in the chosen Vero cell line. With superparamagnetic IONPs applied in 500 µg/ml dose, the viability of murine macrophage cells (J774) was reduced from 75% to 60% in six hours (Naqvi et al, 2010). Our results, covering a wider, possibly more realistic dose range and exposure time range, also indicated cytotoxicity. In contrast to that, Soenen et al (2011) examined four different types of coated IONPs, using the lactate dehydrogenase assay on C17.2 cells, and found no acute toxicity. Similarly, Ying and Hwang (2010) also reported that modification in the surface coating could overcome the cytotoxicity of IONPs. The role of the NPs' chemical composition (possibly, of the dissolved components) was shown by e.g. Fahmy et al (2009) who found that CuO but not Fe₂O₃ or SiO₂ NPs induced cytotoxicity in HEP-2.

Jing et al (2010) showed that on concomitant treatment with daunorubicin (or adriamycin) and IONPs, the proliferation of Raji cells was markedly inhibited. Their results promote a potential clinical application for IONPs in combination with different chemotherapeutics against lymphoma – provided the toxic effect can be focused on the target cells.

Our Ames test data indicated no mutagenicity of the various concentrations of IONPs in the tester strains of *S. typhimurium* TA100, TA98, TA1535, TA1537 and *E. coli* WP2uvrA, with or without metabolic activation.

This result is in line with a literature data on the mutagenic potential of metal oxides NPs. No mutagenic activity of Al₂O₃, Co₃O₄, TiO₂, and ZnO NPs to *S. typhimurium* TA97a, TA100, and *E. coli* WP2 trp uvrA was found, both in absence and presence of S9 mixture (Pan et al, 2010). Likewise, Al₂O₃ (30 nm and 40 nm) did not show mutagenicity in the tester strains of *S. typhimurium* TA100, TA1535, TA98, TA97a and TA102 (Balasubramanyam et al, 2010). Kim et al (2009) reported that Al₂O₃ NPs were not mutagenic on cultured mammalian cells examined with the mouse lymphoma assay (MLA). Yoshida et al (2009) investigated ZnO NPs capped with tetramethylammonium hydroxide and found them non-mutagenic in the Ames test using *S. typhimurium* strains TA98, TA100, TA1535, TA1537 and *E. coli* WP2uvrA strains with and without S9 mixture. Others, however, found certain NPs mutagenic. Iron-platinum (FePt) NPs tested were, with and without S9 mixture, weakly positive in the Ames test on *Salmonella* TA100 strain (Maenosono et al, 2007). Kumar et al (2011) showed mutagenicity of TiO₂ NPs, both in presence and absence of metabolic activation. They also demonstrated the uptake of ZnO and TiO₂ NPs in *S. typhimurium* (TA98 and TA1537) and the NPs' weak mutagenic potential leading to frameshift mutations.

In conclusion, the results of this work and the questions pointed out as aims of the study can be answered as follows:

- 1) Acute intratracheal application of iron oxide nanoparticles had evident general toxic effect (altered body and lung weights) and caused morphological changes in the treated rats' lungs.
- 2) Nanoparticles which reached the lower airways proved to be immunosuppressive: there was decreased immunoglobulin level (IgM and IgG) in the peripheral bronchioles. However, two components of pulmonary redox system (GSH and EC-SOD) did not change, therefore further examination is required.
- 3) The nanoparticles caused irreversible injury to the membranes of alveolar cells. Human A549 cells were more sensitive than animal cells. Our results showed connection between damage of lung cells and production of chemokines (significantly elevated MCP-1 and MIP-1 α levels were measured from the supernatant of treated lung cells). The alveolar epithelial cells could produce chemokines through which they may regulate inflammatory and immune responses in the alveolar microenvironment. The iron oxide NPs had moderate cytotoxic effect on Vero cell line.
- 4) No mutagenic activity could be observed in the bacterial reverse mutation (Ames) test.
- 5) The new, complex experimental model, comprising both *in vivo* and *in vitro* investigations, proved to be suitable for early detection of (previously unknown or partially documented) toxic effects of iron oxide NPs, and for revealing certain connections between the individual toxic effects.

Our results underline the importance and necessity of further long term toxicological experiments. Toxicology studies are the basis for save of human health and the environment relating to nanotechnology. From the research presented in this study, the need for more toxicological examination on nanoparticles is clear. In addition to animal experiments, there is a need to develop and use better and rapid screening tests. *In vitro* studies are likely to provide initial data on nanoparticles, with the findings having to be followed up by *in vivo* studies in animal.

5 REFERENCES

1. Ádám V, Faragó A, Machovich R, Mandl J. 1996. A hemoglobin és a mioglobin (1.3). Porfirin–anyagcsere (2.4). In: Orvosi biokémia, Semmelweis Kiadó. 37-40, 187-229.
2. Ahamed M. 2011. Toxic response of nickel nanoparticles in human lung epithelial A549 cells. *Toxicol in Vitro* 25:930-936.
3. Ames BN, McCann J, Yamasaki E. 1975. Methods for detecting carcinogens and mutagens with the *Salmonella*/mammalian–microsome mutagenicity test. *Mutat Res* 31:347-364.
4. Anderson ME. 1985. Determination of glutathione and glutathione disulphide in biological samples. *Method Enzymol* 113:548-555.
5. Aoki H, Otaka Y, Igarashi K, Takenaka A. 2002. Soy protein reduces paraquat–induced oxidative stress in rats. *J Nutr* 132:2258-2262.
6. Arora S, Rajwade JM, Paknikar KM. 2012. Nanotoxicology and in vitro studies: The need of the hour. *Tox App Pharm* 258:151-165.
7. Bahadur D, Giri J. 2003. Biomaterials and magnetism. *Sadhana* 28:639-656.
8. Balasubramanyam A, Sailaja N, Mahboob M, Rahman MF, Hussain SM, Grover P. 2010. In vitro mutagenicity assessment of aluminium oxide nanomaterials using the *Salmonella*/microsome assay. *Toxicol in Vitro* 24:1871-1876.
9. Bazin H, Beckers A, Querinjean P. 1974. Three classes and four (sub)classes of rat immunoglobulins: IgM, IgA, IgE and IgG1, IgG2a, IgG2b, IgG2c. *Eur J Immunol* 4:44-48.
10. Borm PJ, Robbins D, Haubold S, Kuhlbusch T, Fissan H, Donaldson K, et al. 2006. The potential risks of nanomaterials: a review carried out for ECETOC. Part *Fibre Toxicol* 3:11.
11. Brandenberger C, Rothen-Rutishauser B, Mühlfeld C, Schmid O, Ferron GA, Maier KL, et al. 2010. Effects and uptake of gold nanoparticles deposited at the air–liquid interface of a human epithelial airway model. *Tox App Pharm* 242(1):56-65.
12. Brieland JK, Flory CM, Jones ML, Miller GR, Remick DG, Warren JS, Fantone JC. 1995. Regulation of monocyte chemoattractant proteina-1 gene expression and secretion in rat pulmonary alveolar macrophages by lipopolysaccharide, tumor necrosis factor α and interleukin1b. *Am J Respir Cell Mol Biol* 12:104-109.

13. Brigger I, Dubernet C, Couvreur P. 2002. Nanoparticles in cancer therapy and diagnosis. *Adv Drug Deliv Rev* 54:631-651.
14. Brunauer S, Emmett PH, Teller E. 1938. Adsorption of Gases in Multimolecular Layers. *J Am Chem Soc* 60(2):309-319.
15. Bulte JW, Kraitchman DL. 2004. Iron oxide MR contrast agents for molecular and cellular imaging. *NMR Biomed* 17: 484-499.
16. Clift MJD, Byles MSP, Brown DM, Stone V. 2010. An investigation into the potential for different surface coated quantum dots to cause oxidative stress and affect macrophage cell signalling in vitro. *Nanotoxicology* 4(2):139-149.
17. Cornell RM, Schwertmann U. 2003. The iron oxides – Structure, Properties, reactions, Occurrences and Uses. Wiley–VCH Chapter 1 and 2.
18. Cuenca AG, Jiang H, Hochwald SN, Delano M, Cance WG, Grobmyer SR. 2006. Emerging implications of nanotechnology on cancer diagnostics and therapeutics. *Cancer* 107:459-466.
19. Dhawan A, Sharma V. 2010. Toxicity assessment of nanomaterials: methods and challenges. *Anal Bioanal Chem* 398:589-605.
20. Donaldson K, Stone V, Tran CL, Kreyling W, Borm PJA. 2004. Nanotoxicology. *Occup Environ Med* 61:727-728.
21. Donaldson K, Borm PJ, Castranova V, Gulumian M. 2009. The limits of testing particle-mediated oxidative stress in vitro in predicting diverse pathologies; relevance for testing of nanoparticles. *Part Fibre Tox* 6:13-20.
22. Dura Gy, Szalay B. 2007. Particle exposure through the indoor air environment. In: Simeonova et al (eds.) *Nanotechnology – Toxicological Issues and Environmental Safety*, Springer 271-276.
23. EC COM 338 2004. Communication from the Commission. Towards a European strategy for nanotechnology. Commission of the European Communities. Brussels, 12.5.2004.
24. Fahmy B, Cormier SA. 2009. Copper oxide nanoparticles induce oxidative stress and cytotoxicity in airway epithelial cells. *Toxicol in Vitro* 23:1365-1371.
25. Faraji AH, Wipf P. 2009. Nanoparticles in cellular drug delivery. *Bioorg Chem* 17:2950-2962.
26. Faraji M, Yamini Y, Rezaee M. 2010. Magnetic nanoparticles: synthesis, stabilization, functionalization, characterization, and applications. *J Iran Chem Soc* 7:1-37.

27. Fievet F, Lagier JP, Blin B, Beaudoin B, Figlarz M. 1989. Homogeneous and heterogeneous nucleations in the polyol process for the preparation of micron and submicron size metal particles. *Solid State Ionics* 32:198-205.
28. Fridovich I. 1986. Superoxide dismutases. *Adv Enzymol* 58:61-97.
29. Gilchrist RK, Medal R, Shorey WD, Hanselman RC, Parrott JC, Taylor CB. 1957. Selective inductive heating of lymph nodes. *Ann Surg* 146:596-606.
30. Gonzalez-Flecha B. 2004. Oxidant mechanisms in response to ambient air particles. *Mol Asp Med* 25:169–182.
31. Goshima S, Kanematsu M, Matsuo M, Kondo H, Kato H, Yokoyama R, Hoshi H, Moriyama N. 2004. Nodule-in-nodule appearance of hepatocellular carcinomas: comparison of gadolinium-enhanced and ferumoxides-enhanced magnetic resonance imaging. *J Magn Reson Imaging* 20: 250-255.
32. Gould P. 2006. Nanomagnetism shows in vivo potential. *Nanotoday* 1:34-39.
33. Goya GF, Berquo TS, Fonseca FC, Morales MP. 2003. Static and dynamic magnetic properties of spherical magnetite nanoparticles. *J Appl Phy* 94: 3520-8.
34. Gupta AK, Gupta M. 2005a. Cytotoxicity suppression and cellular uptake enhancement of surface modified magnetic nanoparticles. *Biomater* 26:1565-1573.
35. Gupta AK, Gupta M. 2005b. Synthesis and surface engineering of iron oxide nanoparticles for biomedical applications. *Biomater* 26:3995-4021.
36. Gurzau ES, Neagu C, Gurzau AE. 2003. Essential metals – case study on iron. *Ecotoxicol Environ Safety* 56:190-200.
37. Haschek WM, Witschi H. 1979. Pulmonary fibrosis – a possible mechanism. *Toxicol Appl Pharmacol* 51:475-484.
38. Horváth E, Oszlánzi G, Máthé Zs, Szabó A, Kozma G, Sápi A, et al. 2011. Nervous system effects of dissolved and nanoparticulate cadmium in rats in subacute exposure. *J Appl Toxicol* 31:471-476.
39. Huang YW, Wu CH, Aronstam RS, 2010. Toxicity of transition metal oxide nanoparticles: recent insights from in vitro studies. *Materials* 3:4842-4859.
40. Hurley JF, Cherrie JW, Donaldson K, Seaton A, Tran CL. 2003. Assessment of health effects of long-term occupational exposure to tunnel dust in the London Underground. Institute of Occupational Medicine Research Report TM/03/02.

41. Ito A, Honda H, Kobayashi T. 2006. Cancer immuno-therapy based on intracellular hyperthermia using magnetite nanoparticles: a novel concept of "heat-controlled necrosis" with heat shock protein expression. *Cancer Immunol Immunother* 55:320-328.
42. Ito A, Shinkai M, Honda H, Kobayashi T. 2005. Medical application of functionalized magnetic nanoparticles. *J Biosci Bioeng* 100:1-11.
43. Jing H, Wang J, Yang P, Ke X, Xia G, Chen B. 2010. Magnetic Fe₃O₄ nanoparticles and chemotherapy agents interact synergistically to induce apoptosis in lymphoma cells. *Int J Nanomed* 5:999-1004.
44. Johannsen M, Gneveckow U, Eckelt L, Feussner A, Waldofner N, Scholz R, Deger S, Wust P, Loening SA, Jordan A. 2005. Clinical hyperthermia of prostate cancer using magnetic nanoparticles: presentation of a new interstitial technique. *Int J Hyperthermia* 21:637-647.
45. Kamat PV, Huehn R, Nicolaescu R. 2002. A "sense and shoot" approach for photocatalytic degradation of organic contaminants in water. *J Physical Chemistry B* 106(4):788-794.
46. Kamat PV, Meisel D. 2003. Nanoscience opportunities in environmental remediation. *Compt Rend Chim* 6(8-10):999-1007.
47. Karlsson HL, Holgersson A, Moller L. 2008. Mechanisms related to the genotoxicity of particles in the subway and from other sources. *Chem Res Toxicol* 21:726-31.
48. Kim YJ, Choi HS, Song MK, Youk DY, Kim JH, Ryu JC. 2009. Genotoxicity of aluminum oxide (Al₂O₃) nanoparticle in mammalian cell lines. *Mol Cell Toxicol* 5:172-178.
49. Kirkland, D.J. 1994. Statistical Evaluation of Mutagenicity Test Data: Recommendations of the U.K. Environmental Mutagen Society. *Environ Health Persp* 102(1):43-47
50. Kovacs EJ, Dipietro LA. 1994. Fibrogenic cytokines and connective tissue production. *FASEB J* 8:854-861.
51. Kumar A, Pandey AK, Singh SS, Shanker R, Dhawan A. 2011. Cellular uptake and mutagenic potential of metal oxide nanoparticles in bacterial cells. *Chemosphere* 83:1124-1132.
52. Kumar CSSR, Mohammad F. 2011. Magnetic nanomaterials for hyperthermia-based therapy and controlled drug delivery. *Advanced Drug Delivery Reviews* 63:789-808.

53. Laurent S, Forge D, Port M, Roch A, Robic C, Vander Elst L, et al. 2008. Magnetic iron oxide nanoparticles: synthesis, stabilization, vectorization, physicochemical characterizations, and biological applications. *Chem Rev* 108:2064-110.
54. Lead JR, Smith E. 2009. Environmental and Human Health Impacts of Nanotechnology (Chapter 1.8.1). Wiley, UK. Chapter 1.
55. Lee MH, Cho K, Shah AP, Biswas P. 2005. Nanostructured Sorbents for Capture of Cadmium Species in Combustion Environments. *Environ Sci Technol* 39(21):8481-8489.
56. Lowry OH, Rosebrough NJ, Farr AL, Randall RJ. 1951 Protein measurement with the Folin-Phenol reagents. *J Biol Chem* 193:265-275.
57. Maenosono S, Suzuki T, Saita S. 2007. Mutagenicity of water-soluble FePt nanoparticles in Ames test. *J Toxicol Sci* 32:575-9.
58. Mahmoudi M, Simchi A, Imani M, Shokrgozar MA, Milani AS, Häfeli UO, Stroeve P. 2010. A new approach for the in vitro identification of the cytotoxicity of superparamagnetic iron oxide nanoparticles. *Colloid Surface B: Biointerfaces* 75:300-309.
59. Maron DM, Ames BN. 1983. Revised methods for the salmonella mutagenicity test. *Mutat Res* 113:173-215.
60. Maynard AD, Aitken RJ, Butz T, Colvin V, Donaldson K, Oberdörster G, et al. 2006. Safe handling of nanotechnology. *Nature* 444:267-9.
61. McBain SC, Yiu HH, Dobson J. 2008. Magnetic nanoparticles for gene and drug delivery. *Int J Nanomed* 3:169-180.
62. Meister A, Anderson ME. 1983. Glutathione. *Annu Rev Biochem* 52:711-760.
63. Mornet S, Vasseur S, Grasset F, Duguet E. 2004. Magnetic nanoparticle design for medical diagnosis and therapy. *J Mater Chem* 14:2161-2175.
64. Muller J, Huaux F, Moreau N, Misson P, Heilier JF, Delos M, et al. 2005. Respiratory toxicity of multi-wall carbon nanotubes. *Toxicol Appl Pharm* 207:221-231.
65. Naqvi S, Samim M, Abdin MZ, Ahmed FJ, Maitra AN, Prashant CK, Dinda AK. 2010. Concentration-dependent toxicity of iron oxide nanoparticles mediated by increased oxidative stress. *Int J Nanomed* 5:983-989.
66. Oberdörster G, Elder A, Rinderknecht A. 2009. Nanoparticles and the brain: cause for concern? *J Nanosci Nanotechnol* 8:4996-5007.

67. Oberdörster G, Oberdörster E, Oberdörster J. 2005. Nanotoxicology: an emerging discipline evolving from studies of ultrafine particles. *Environ Health Perspect* 113:823-839.
68. OECD 1997. (Organisation for Economic Cooperation and Development) Guideline for the testing of chemicals: bacteria reverse mutation test. Guideline 471.
69. Oszlánzi G, Horváth E, Szabó A, Horváth E, Sápi A, Kozma G, et al. 2010. Subacute exposure of rats by metal oxide nanoparticles through the airways: general toxicity and neuro-functional effects. *Acta Biol Szegediensis* 54(2):165-170.
70. Paine R, Rolfe MW, Standiford TK, Burdick MD, Rollins BJ, Strieter RM. 1993. MCP-1 expression by rat type II alveolar epithelial cells in primary culture . *J Immunol* 150:4561-4570.
71. Pan X, Redding JE, Wiley PA, Wena L, McConnell JS, Zhang B. 2010. Mutagenicity evaluation of metal oxide nanoparticles by the bacterial reverse mutation assay. *Chemosphere* 79:113-116.
72. Parkes WR. 1982. Occupational Lung Disorders. In: *Inert Dusts*. Butterworths, London-Boston-Sydney-Wellington-Durban-Toronto. pp.113-133.
73. Paur HR, Cassee FR, Teeguarden J, Fissan H, Diabate S, Aufderheide M, Kreyling WG, et al. 2011. In-vitro cell exposure studies for the assessment of nanoparticle toxicity in the lung—A dialog between aerosol science and biology. *J Aerosol Sci* 42:668-692.
74. PEN 2005. The project on emerging nanotechnologies. www.nanotechproject.org
75. REACH 2006. http://ec.europa.eu/environment/chemicals/reach/reach_intro.htm
76. Rezin GT, Cardoso MR, Goncalves CL, Scaini G, Fraga DB, Riegel RE, et al. 2008. Inhibition of mitochondrial respiratory chain in brain of rats subjected to an experimental model of depression. *Neurochem Int* 53:395-400.
77. Richards RJ, Davies N, Atkins J, Oreffo VIC. 1987. Isolation, biochemical characterisation and culture of lung type II cells of the rat. *Lung* 165(1):143-158.
78. Roco MC, Bainbridge WS. 2003. *Converging technologies for improving human performance: nanotechnology, biotechnology, information technology and cognitive science*. Kluwer Academic Publishers, New York.
79. Roco MC. 2005. International Perspective on Government Nanotechnology Funding in 2005. *J Nanopart Res* 7:707-712.

80. RSRAE 2004. Royal Society and Royal Academy of Engineering Report, Nanoscience and Nanotechnologies: Opportunities and Uncertainties. In <<http://www.nanotec.org.uk/finalReport.htm>>.
81. Sárközi L, Horváth E, Kónya Z, Kiricsi I, Szalay B, Vezér T, Papp A. 2009. Subacute intratracheal exposure of rats to manganese nanoparticles: Behavioral, electrophysiological, and general toxicological effects. *Inhal Toxicol* 21(S1):83-91.
82. Sayes CM, Reed KL, Warheit DB. 2007. Assessing toxicity of fine and nanoparticles: comparing in vitro measurements to in vivo pulmonary toxicity profiles. *Toxicol Sci* 97:163-180.
83. Schärer K. 1977. The effect of chronic underfeeding on organ weights of rats. *Toxicology* 7:45-56.
84. Schlorf T, Meincke M, Kossel E, Glüer CC, Jansen O, Mentlein R. 2011. Biological Properties of Iron Oxide Nanoparticles for Cellular and Molecular Magnetic Resonance Imaging. *Int J Mol Sci* 12:12-23.
85. Sharon N, Lis H. 1989. Lectins as cell recognition molecules. *Science* 246:227-234.
86. Singh N, Jenkins GJS, Asadib R, Doak SH. 2010. Potential toxicity of superparamagnetic iron oxide nanoparticles (SPION). *Nano Reviews* 1:5358 – DOI: 10.3402/nano.v1i0.5358.
87. Smith RE, Strieter RM, Zhang K, Phan SH, Standiford TJ, Lukacs NW, Kunkel SL. 1995. A role for C–C chemokines in fibrotic lung disease. *J Leukocyte Biol* 57:782-787.
88. Soenen SJH, Himmelreich U, Nuytten N, De Cuyper M. 2011. Cytotoxic effects of iron oxide nanoparticles and implications for safety in cell labelling. *Biomaterials* 32:195-205.
89. Suh WH, Suslick KS, Stucky GD, Suh YH. 2009. Nanotechnology, nanotoxicology, and neuroscience *Prog Neurobiol* 87:133-170.
90. Tátrai E, Ungváry Gy, Adamis Z. 1994. On the structural differences in the membranes between ciliated bronchial and non-ciliated lymphoepithelium in rats. *Eur J Histochem* 38:59-64.
91. Taylor K, Gordon N, Langley G, Higgings W. 2008. Estimates for Worldwide Laboratory Animal Use in 2005. *Alternatives for Laboratory Animals* 36:327-342.
92. Tyner KM, Schiffman SR, Giannelis EP. 2004. Nanobiohybrids as delivery vehicles for camptothecin. *J Control Release* 95:501-514.

93. Vigor K, Kyrtatos P, Minogue S, Kallumadil, Al-Jamal K, Kogelberg H, et al. 2010. Nanoparticles functionalised with recombinant single chain Fv antibody fragments (scFv) for the magnetic resonance imaging of cancer cells. *Biomaterials* 31:1307-1315.
94. Warheit DB, Sayes CM, Reed KL, Swain KA. 2008. Health effects related to nanoparticle exposures: Environmental, health and safety considerations for assessing hazards and risks. *Pharmacol Therapeutics* 120:35-42.
95. Ying E, Hwang H. 2010. In vitro evaluation of the cytotoxicity of iron oxide nanoparticles with different coatings and different sizes in A3 human T lymphocytes. *Sci Total Environ* 408:4475-4481.
96. Yoshida R, Kitamura D, Maenosono S. 2009. Mutagenicity of water-soluble ZnO nanoparticles in Ames test. *J Toxicol Sci* 34:119-122.
97. Zee van der J. 2002. Heating the patient: a promising approach? *Annals Oncol* 13:1173-1184.
98. Zonghuan L, Malcolm PD, Zhanhu G, Vladimir GO, Kumar CSSR, Yuri LM. 2005. Magnetic switch of permeability for polyelectrolyte microcapsules embedded with nanoparticles. *Langmuir* 21:2042-2050.

6 ACKNOWLEDGEMENT

I would like to thank to Prof. Dr. László Nagymajtényi, Head of the Department of Public Health and Dr. Gyula Dura, Head of National Institute of Environmental Health for the opportunity to do experimental work and prepare my PhD thesis.

I am especially thankful to my supervisor, Dr. Tünde Vezér for all her help and Dr. Erzsébet Tátrai for her advice and support throughout my PhD. In particular I would like to thank Dr. András Papp for his helpful discussions and comments.

I would like to thank to my colleagues for their ongoing help, technical support and work. The staff of Department of Public Health, University of Szeged, and the staff of Department of Toxicology, National Institute of Environmental Health for their help in the research.

Thanks also goes to the National Centre for Epidemiology for providing Vero cells, to Dr Elena Alina Palade (Szent István University, Budapest) for TEM photography, to Dr. Géza Török and Dr. Tamás Pándics for their valuable comments and suggestions.

Finally, I would like to thank my family and my friends for constant encouragement and for always being there.

7 APPENDIX

Dura Gy, Szalay B. Particle exposure through indoor environment. **Nanotechnology – Toxicological Issues and Environmental Safety**, Springer. 2007. pp 271-276.

Szalay B, Kováčikova Z, Brózik M, Pándics T, Tátrai E. Effects of iron oxide nanoparticles on pulmonary morphology, redox system, production of immunoglobulins and chemokins in rats: In vivo and In vitro studies. **Central European Journal of Occupational and Environmental Medicine** 2008. 14(2):149-164.

Szalay B, Kováčiková Z, Brózik M, Pándics T, Tátrai E. Vas-oxid nanorészecskék tüdőtoxicitása. **Egészségtudomány** 2009. LIII(1):103-115.

Szalay B, Tátrai E, Pándics T, Dura Gy. Nikkel-, vas- és cinkoxid nanopartikulumok tüdősejtekre gyakorolt membránkárosító hatása. **Egészségtudomány** 2010. LIV (1):52-60.

Szalay B, Vezér T. In vitro mutagenicity evaluation of iron oxide nanoparticles by the bacterial reverse mutation assay. **XVII. International Symposium on Analytical and Environmental Problems**. (Galbács Z., ed.) Szeged, 2011. pp. 275-278.

Szalay B, Tátrai E, Nyíró G, Vezér T, Dura Gy. Potential toxic effects of iron oxide nanoparticles in in vivo and in vitro experiments. **Journal of Applied Toxicology** 2011. DOI 10.1002/jat.1779.